© 2018. Published by The Company of Biologists Ltd | Development (2018) 145, dev160184. doi:10.1242/dev.160184

RESEARCH ARTICLE

A blood capillary plexus-derived population of progenitor cells contributes to genesis of the dermal lymphatic vasculature during embryonic development

Cathy Pichol-Thievend[1], Kelly L. Betterman[2], Xiaolei Liu[3], Wanshu Ma[3], Renae Skoczylas[1], Emmanuelle Lesieur[1], Frank L. Bos[4,*], Dorte Schulte[5], Stefan Schulte-Merker[5], Benjamin M. Hogan[1], Guillermo Oliver[3], Natasha L. Harvey[2,‡,§] and Mathias Francois[1,‡,§]

ABSTRACT

Despite the essential role of the lymphatic vasculature in tissue homeostasis and disease, knowledge of the organ-specific origins of lymphatic endothelial progenitor cells remains limited. The assumption that most murine embryonic lymphatic endothelial cells (LECs) are venous derived has recently been challenged. Here, we show that the embryonic dermal blood capillary plexus constitutes an additional, local source of LECs that contributes to the formation of the dermal lymphatic vascular network. We describe a novel mechanism whereby rare PROX1-positive endothelial cells exit the capillary plexus in a *Ccbe1*-dependent manner to establish discrete LEC clusters. As development proceeds, these clusters expand and further contribute to the growing lymphatic system. Lineage tracing and analyses of *Gata2*-deficient mice confirmed that these clusters are endothelial in origin. Furthermore, ectopic expression of *Vegfc* in the vasculature increased the number of PROX1-positive progenitors within the capillary bed. Our work reveals a novel source of lymphatic endothelial progenitors employed during construction of the dermal lymphatic vasculature and demonstrates that the blood vasculature is likely to remain an ongoing source of LECs during organogenesis, raising the question of whether a similar mechanism operates during pathological lymphangiogenesis.

KEY WORDS: Lymphatic endothelial cells, Skin, Lymphangiogenesis, PROX1, Lineage tracing, Progenitor cell, Mouse genetics

INTRODUCTION

The cellular origin of the lymphatic vascular network has long been debated. Over the last decade, studies in the mouse embryo concluded that most, if not all, embryonic lymphatic endothelial cells (LECs) derive from the cardinal veins (CVs) and intersomitic veins (ISVs) during development (Srinivasan et al., 2007; Yang et al., 2012). This venous contribution was validated in zebrafish (Koltowska et al., 2015; Nicenboim et al., 2015; Okuda et al., 2012). By contrast, studies performed in frogs and birds indicated that additional sources of LECs contribute to the genesis of the lymphatic vasculature during development (Ny et al., 2005; Schneider et al., 1999; Wilting et al., 2006). Recent work performed in mouse models also suggested that non-venous sources of LECs contribute in limited numbers to the genesis of the lymphatic vasculature in skin, heart and intestine (Klotz et al., 2015; Martinez-Corral et al., 2015; Stanczuk et al., 2015).

During mouse embryonic development, the first wave of LEC specification starts at ∼9.5 days post-coitum (dpc). A pool of LEC progenitor cells, identified by their expression of the homeobox transcription factor gene *Prox1* (Wigle and Oliver, 1999), is first observed in the CVs at ∼9.5 dpc. These LEC progenitors subsequently exit the veins and migrate in a dorsolateral direction to generate an initial lymphatic vascular plexus and lymph sacs (François et al., 2012; Hägerling et al., 2013; Yang et al., 2012). Advances in high-resolution imaging techniques have allowed for a better description of these early stages of lymphatic vascular development (François et al., 2012; Hägerling et al., 2013; Yang et al., 2012). However, there is still a gap in our knowledge regarding the cellular mechanisms by which these initial lymphatic structures subsequently give rise to unique, organ-specific networks that fulfil tissue-specific functions.

As mentioned above, recent findings challenged the proposal that all mammalian LECs are derived from the progenitor pool specified in the cardinal and intersomitic veins. In particular, two studies argued that some lymphatic vessels of the gut arise from origins distinct from the major venous reservoir of LEC progenitors (Mahadevan et al., 2014; Stanczuk et al., 2015). In the first report, *Pitx2*-dependent arterial development was shown to initiate the assembly of a non-venous-derived lymphatic vascular structure that subsequently connected with a venous-derived population of LECs to generate mesenteric lymphatic vessels (Mahadevan et al., 2014). In the second study, genetic lineage-tracing experiments revealed that c-KIT (KIT)-positive haemogenic endothelium provides an additional source of mesenteric LECs that, combined with a venous-derived pool, generates an interconnected mesenteric lymphatic vessel network (Stanczuk et al., 2015). Investigation of *Vegfr3*$^{+/-}$;*p110α*$^{+/-}$ mice provided further evidence of the contribution of two distinct progenitor pools to the mesenteric lymphatic vasculature; these analyses revealed that the development of the mesenteric lymphatic system was profoundly impaired in *Vegfr3*$^{+/-}$;*p110α*$^{+/-}$

[1]Institute for Molecular Bioscience, The University of Queensland, Brisbane, QLD 4072, Australia. [2]Centre for Cancer Biology, University of South Australia and SA Pathology, Adelaide 5001, South Australia, Australia. [3]Center for Vascular and Developmental Biology, Feinberg Cardiovascular Research Institute, Northwestern University, Chicago, IL 60611, USA. [4]Hubrecht Institute, Royal Netherlands Academy of Arts and Sciences (KNAW) and University Medical Centre, Utrecht 3584CT, The Netherlands. [5]University of Münster, 48149 Münster, Germany Institute for Cardiovascular Organogenesis and Regeneration, Faculty of Medicine, Westfälische Wilhelms-Universität Münster (WWU), Mendelstrasse 7, 48149 Münster and CiM Cluster of Excellence, Germany.
*Present address: Princess Máxima Center for Pediatric Oncology, Utrecht 3584CT, The Netherlands.
‡These authors contributed equally to this work

§Authors for correspondence (natasha.harvey@unisa.edu.au; m.francois@imb.uq.edu.au)

N.L.H., 0000-0002-3461-9376; M.F., 0000-0002-9846-6882

Received 5 October 2017; Accepted 20 April 2018

Development (2018) 145, dev160184. doi:10.1242/dev.160184

mice, whereas development of the dermal lymphatic vasculature was not (Stanczuk et al., 2015). Recent work investigating development of the cardiac lymphatic vasculature also suggested that a hybrid mechanism of lymphatic vessel genesis is employed in the heart, with yolk sac (YS) haemogenic endothelium proposed as a second source of a small population of cardiac LECs (Klotz et al., 2015). Finally, up to one-third of dermal lymphatic vessels in the lumbar and dorsal midline regions of the embryonic mouse skin were also proposed to derive from a non-venous origin, although the cellular source of these cells was not identified (Martinez-Corral et al., 2015).

Here, using a combination of genetic lineage tracing, endothelial-specific targeted gene disruption and gain of function, and high-resolution imaging, we report a novel mechanism by which a subpopulation of dermal LECs in the dorso-cervical region of the mouse embryo arises from a local blood vascular origin. These LEC progenitors are first observed during a narrow time window (13.5-16.5 dpc) as PROX1-positive cells within the dermal capillary plexus close to the embryonic midline. Subsequently, these cells physically disconnect from the blood vasculature as single cells or small clusters. Upon exit from the capillary bed, these cells increase expression of LEC markers, including VEGFR3 (FLT4) and neuropilin 2 (NRP2), and acquire specific LEC markers such as podoplanin (PDPN). Cells within LEC clusters proliferate to form larger groups of cells before merging with pre-existing lymphatic vessels that sprout from the jugular region towards the embryonic midline. Fate-mapping analyses confirmed the blood vascular endothelial origin of this discrete population of progenitor cells. Moreover, the emergence of LEC progenitors from the capillary plexus is dependent on *Ccbe1*, as indicated by the observation that *Ccbe1* null embryos retain PROX1-positive cells within the capillary plexus, genetically confirming their blood vascular origin. By employing a novel endothelial-specific VEGFC gain-of-function (VegfcGOF) model system, we demonstrate that the number of PROX1-positive cells in the capillary plexus is regulated by VEGFC; *Tie2-Cre;VegfcGOF* embryos exhibit a dramatically increased number of PROX1-positive cells within the capillary bed. These data suggest either that VEGFC promotes the specification of LEC progenitors in the capillary plexus, or that VEGFC promotes LEC progenitor cell proliferation. We propose that the transient specification of LEC progenitors in the dermal capillary network in the midline region of the mouse embryo provides an additional source of LECs employed during construction of the lymphatic vasculature in the skin. Such a mechanism potentially facilitates a more rapid expansion of an interconnected network than a mechanism relying on centrifugal sprouting alone. Our work re-defines the embryonic developmental window during which blood vessels provide a source of LECs and has implications for the mechanisms underlying lymphangiogenesis in pathological settings, including the tumour microenvironment and inflammation.

RESULTS

Characterisation of discrete LEC clusters during embryonic dermal lymphangiogenesis

During the course of our studies investigating morphogenesis of the dermal lymphatic vasculature in the mouse embryo between 13.5 and 16.5 dpc, we noticed that in addition to a connected plexus of lymphatic vessels sprouting from the flanks toward the embryonic midline, discrete clusters and larger 'islands' of LECs were apparent in the midline region (Fig. 1A, arrows). Analysis of PROX1, NRP2, VEGFR3 and PDPN demonstrated that isolated cell clusters express all of these markers, validating their lymphatic identity (Fig. 1A,C, Fig. S1A). The presence of isolated groups of LECs throughout the cervico-thoracic region in the midline prompted us to investigate whether there could be multiple mechanisms involved in building a connected functional dermal lymphatic vascular plexus during development.

In order to characterise the LEC clusters in greater detail, we performed a comprehensive quantitative analysis of cell number per cluster, together with a qualitative analysis of LEC identity at multiple stages of development. To enumerate clusters, we chose to focus on small groups of LECs consisting of a maximum of four cells per cluster. This number of cells per cluster was selected on the basis that two rounds of cell division would occur from one LEC progenitor to generate a four-cell cluster facilitating the identification of clusters in the early stages of their formation. The number of these small clusters decreased between 13.5 and 16.5 dpc, suggesting that small clusters correspond to a transient intermediate state during network assembly (Fig. 1A,B left). The number of cells per cluster increased between 13.5 and 16.5 dpc, suggesting that cells within clusters undergo proliferation (Fig. 1B right, C). To investigate this proliferative potential, LEC division was measured by co-staining for PROX1, NRP2 and 5-ethynyl-2′-deoxyuridine (EdU) incorporation. Co-staining of PROX1-positive cells with EdU confirmed that cells within clusters actively proliferate (Fig. 1C, arrows) and revealed some instances of PROX1-positive LECs undergoing mitosis (Fig. 1C, blue arrow, anaphase stage). We also observed that the number of cells per cluster was variable within skin samples at any given time point analysed (Fig. 1B,C), suggesting that cluster formation is an ongoing process that occurs within a developmental window between 13.5 dpc and 16.5 dpc. High-resolution imaging analysis of cluster morphology revealed filopodial extensions between adjacent LEC clusters and between LEC clusters and sprouting lymphatic vessels (Fig. S1C, arrows). This interplay suggests that LEC clusters are likely to be incorporated into the main lymphatic vascular network, in a similar fashion to the proposed mechanism of postnatal development of the meningeal lymphatic vasculature (Antila et al., 2017).

Dermal LEC clusters have an endothelial origin

Recent studies have proposed alternative sources of LECs that contribute to distinct tissues during mouse embryonic development (Klotz et al., 2015; Mahadevan et al., 2014; Stanczuk et al., 2015). During skin organogenesis, a non-venous source for a fraction of the lymphatic vasculature has been suggested, but has remained elusive (Klotz et al., 2015; Martinez-Corral et al., 2015; Stanczuk et al., 2015). In order to identify the cellular origin of dermal LEC clusters, we employed a genetic lineage-tracing approach. We first assessed the involvement of endothelial cells using two complementary endothelial-specific Cre lines: *Sox18-CreERT2* (McMahon et al., 2008) and *Cdh5-CreERT2* (Wang et al., 2010), both of which were crossed with tdTomato reporter mice (Madisen et al., 2010). Following the administration of a single dose of tamoxifen at 9.5 dpc to induce Cre activity, the time at which LECs are first specified in the CV, whole-mount immunostaining of 14.5 dpc skin was performed using antibodies for PROX1 and NRP2 to identify all LECs. Analysis of immunostaining revealed that 51% of LEC clusters were labelled by *Sox18-CreERT2* (n=8 embryonic skins) and 74% of LEC clusters were labelled by *Cdh5-CreERT2* (n=6 embryonic skins) (Fig. 2A,B). The percentage of tdTomato-positive LECs in the major pre-existing lymphatic network correlated with the percentage of tdTomato-positive LEC clusters for both lines (46% versus 51% using *Sox18-CreERT2* and 69% versus 74%

Development (2018) 145, dev160184. doi:10.1242/dev.160184

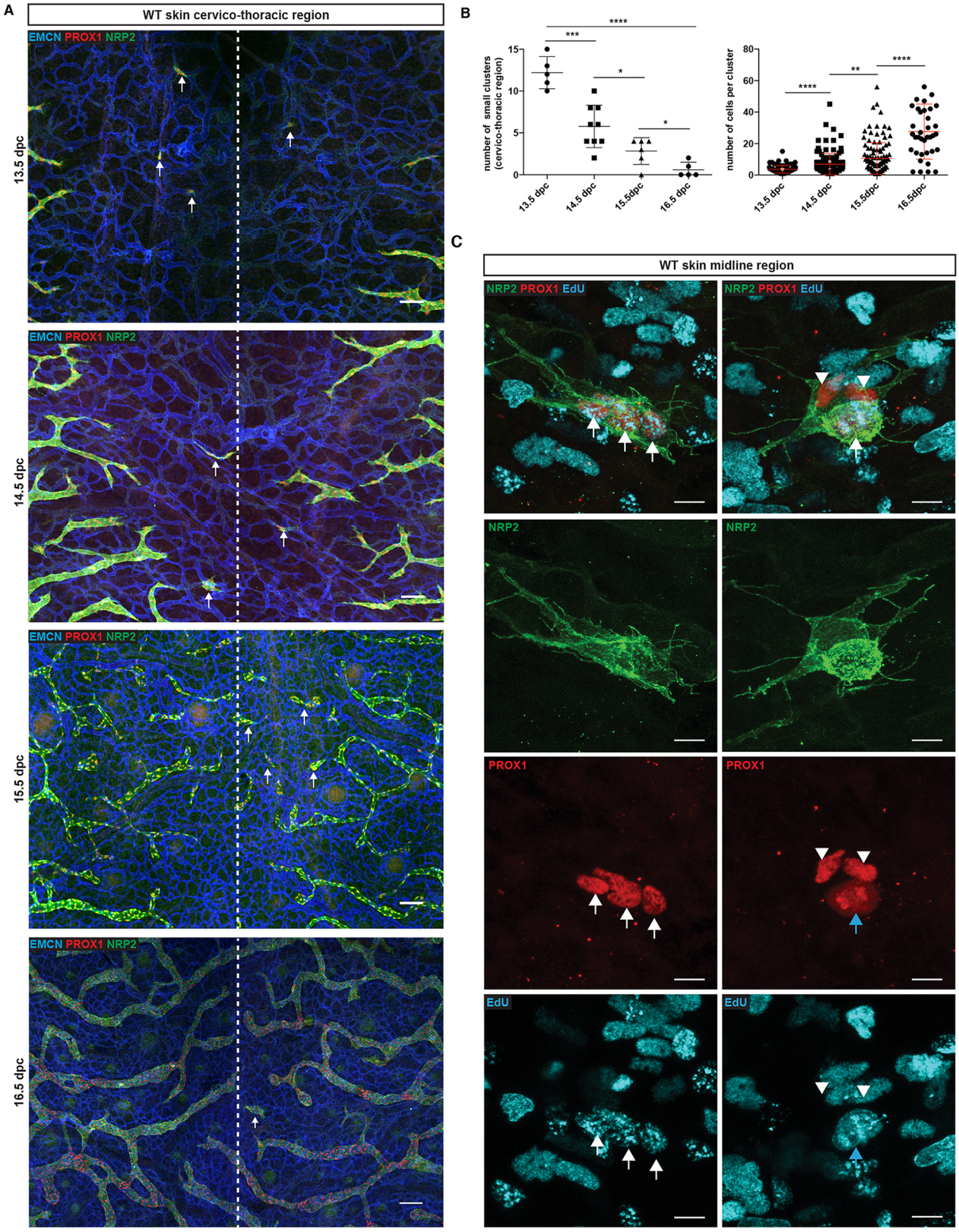

Fig. 1. Characterisation of a discrete population of LECs during embryonic skin development. (A) Whole-mount immunostaining of wild-type (WT) embryonic skin at the indicated time points. Blood vessels are stained with EMCN (blue) and lymphatic vessels with neuropilin 2 (NRP2, green) and PROX1 (red). The dashed line represents the midline of the embryo. Arrows indicate isolated LEC clusters. (B) Left: Number of small LEC clusters (maximum of four cells per cluster) per skin sample. Error bars represent s.e.m. ****P<0.0001, ***P<0.001, *P<0.05 (unpaired t-test). Right: Number of cells per cluster during development. Error bars represent s.e.m. ****P<0.0001, **P<0.01 (Mann–Whitney test). Left graph: 13.5 dpc (n=5), 14.5 dpc (n=9), 15.5 dpc (n=6), 16.5 dpc (n=5). Right graph:13.5 dpc (n=3) 14.5 dpc (n=5) 15.5 dpc (n=5) 16.5 dpc (n=8). (C) Whole-mount immunostaining of embryonic skin at 14.5 dpc for NRP2 (green), PROX1 (red) and EdU (blue). Arrows indicate proliferating LECs and arrowheads indicate non-proliferating cells. Scale bars: 100 µm (A); 10 µm (C).

Development (2018) 145, dev160184. doi:10.1242/dev.160184

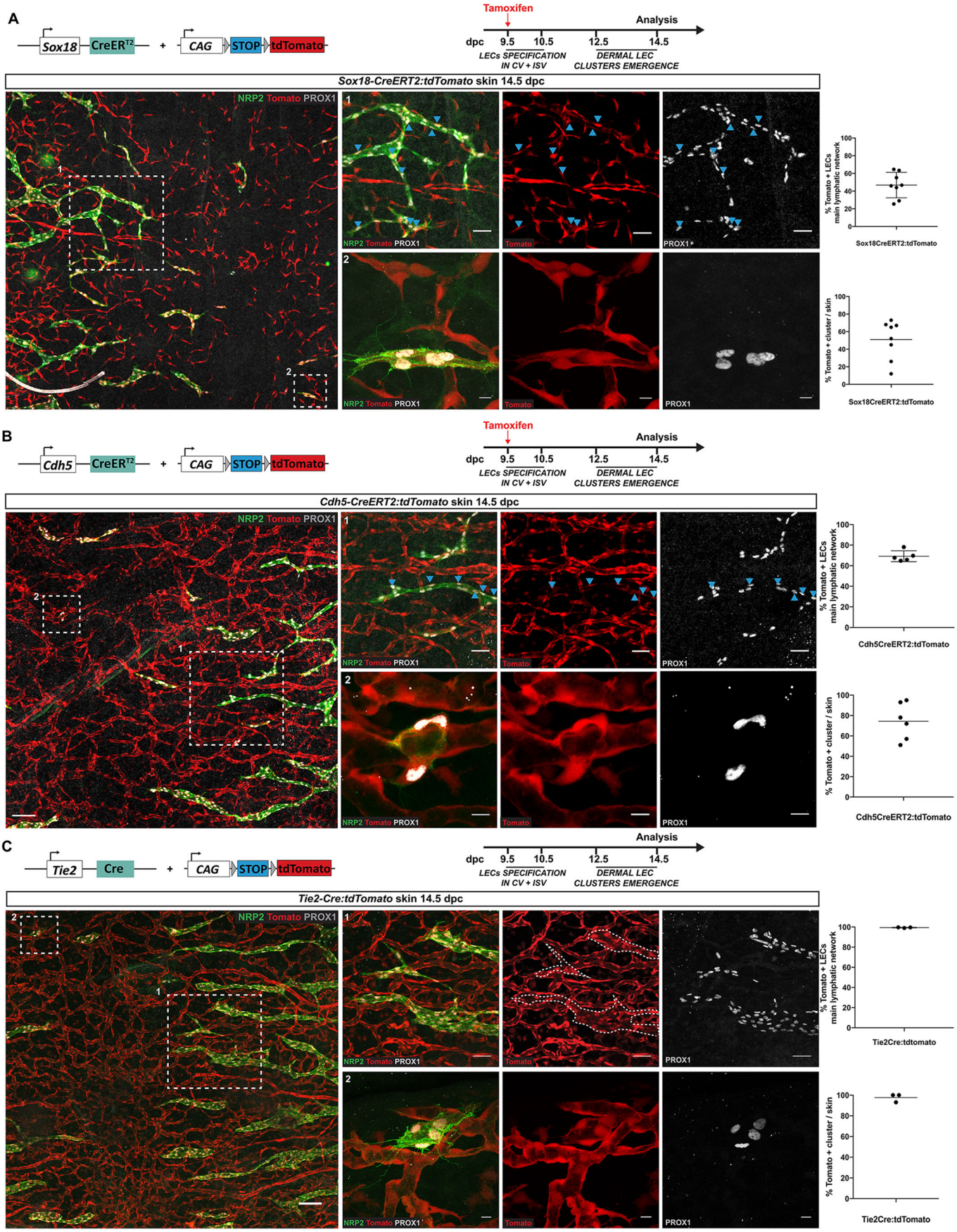

Fig. 2. See next page for legend.

Development (2018) 145, dev160184. doi:10.1242/dev.160184

Fig. 2. Isolated LEC clusters derive from an endothelial origin. (A-C) Whole-mount immunostaining of embryonic skin at 14.5 dpc for NRP2 (green) and PROX1 (grey) for *Sox18-CreERT2:tdTomato* (A), *Cdh5-CreERT2:tdTomato* (B) and *Tie2-Cre:tdTomato* (C) embryos. Blue arrowheads indicate tdTomato-positive LECs. Scale bars: left images (100 µm), panel 1 series (50 µm), panel 2 series (10 µm). Top graphs represent the percentage of tdTomato-positive LECs in the main lymphatic network and bottom graphs represent the percentage of tdTomato-positive LEC clusters in *Sox18Cre-ERT2:tdTomato* (A), *Cdh5-CreERT2:tdTomato* (B) or *Tie2-Cre:tdTomato* (C) skins. *Sox18* (n=8), *Cdh5* (n=6) and *Tie2* (n=3). Error bars represent s.e.m. Schematics of the *Sox18-CreERT2*, *Cdh5-CreERT2*, *Tie2-Cre* transgenes, tdTomato construct and tamoxifen administration schedule are shown at the top of each panel.

using *Cdh5-CreERT2*), suggesting that LEC clusters are derived from an endothelial cell population (Fig. 2A,B, graphs). Furthermore, quantitative analysis of these two inducible lines showed that the embryos with the highest number of tdTomato-positive blood endothelial cells also contained the highest percentage of tdTomato-positive LEC clusters (data not shown), suggesting that the percentage of tdTomato-positive LECs is directly correlated to the level of Cre efficiency. The fact that neither of these Cre lines labelled 100% of blood vascular endothelial cells or LEC clusters, which was likely to be due to incomplete Cre-mediated excision, raised the possibility that a non-endothelial source might also contribute progenitors important for the development of LEC clusters. To bypass Cre mosaicism, we analysed whether a constitutively active *Tie2-Cre:tdTomato* reporter line (Kisanuki et al., 2001) could be used to investigate a potential blood vascular origin of the lymphatic vasculature. To validate the use of *Tie2-Cre*, we assessed GFP levels in the dermal lymphatic vessels of *Tie2-GFP* reporter mice. Immunostaining analyses of skin at 14.5 and 16.5 dpc showed that all dermal lymphatic vessels were negative for GFP, whereas blood vascular endothelial cells were positive (Fig. S2). This observation is consistent with the lack of *Tie2* expression previously reported in the developing lymphatic system (Srinivasan et al., 2007) and supported use of the *Tie2-Cre:tdTomato* line as a tool to analyse the potential contribution of blood vascular-derived progenitors to the dermal lymphatic vasculature. Whole-mount immunostaining of embryonic skin at 14.5 dpc with antibodies to PROX1 and NRP2 demonstrated that 99.4% of LECs in the main lymphatic network and 97.7% of LEC clusters (n=3 embryonic skins) were tdTomato positive, definitively demonstrating that LEC clusters derive from an endothelial origin (Fig. 2C). To elucidate whether the LEC clusters previously observed in the lumbar region of embryonic skin might share a similar blood vascular origin, we analysed tdTomato levels in this anatomical location. tdTomato-positive LEC clusters corresponding to our definition (four cells or fewer) were also observed in similar locations relative to the midline (ahead of the migration front, near the neural tube) in the lumbar region of the embryo (Fig. S3). Based on our observations and in-depth characterisation of cervical LEC clusters, we consider that the cellular origin of cervical and lumbar clusters is likely to be the same.

Dermal LEC clusters do not originate from haemogenic endothelium

To investigate specifically the potential contribution of haemogenic endothelium to LEC cluster formation, we combined two complementary approaches: lineage tracing to map the fate of haemogenic endothelium-derived cells, and analysis of cluster formation in a mouse model lacking haemogenic endothelium. To investigate whether the progeny of haemogenic endothelium contribute to the development of LEC clusters in the skin, *c-Kit-CreERT2* mice (Klein et al., 2013) were crossed with R26R-eYFP reporter mice (Srinivas et al., 2001) and Cre activity was induced by a single dose of tamoxifen at 10.5 dpc. Immunostaining of *c-Kit-CreERT2;ROSA-eYFP* skins at 13.5 dpc did not detect YFP-positive cells within dermal LEC clusters or lymphatic vessels (Fig. 3A, Fig. S4B), although robust YFP labelling of c-KIT-positive haematopoietic cells resident in the skin was observed (Fig. S4A). In accordance with these observations, LEC clusters were also negative for endogenous c-KIT, as well as the haematopoietic progenitor cell markers GATA2 and RUNX1 (Fig. S1B). Importantly, a few YFP-positive cells were detected in mesenteric lymphatic vessels and the mesenteric lymph sac (Fig. S4B, arrows) of the same embryo, as previously reported (Stanczuk et al., 2015). Together, these data suggest that c-KIT-positive haemogenic endothelium is not a source of lymphatic endothelial progenitor cells employed during construction of the dermal lymphatic vasculature.

To investigate further whether haemogenic endothelium contributes to the genesis of the dermal lymphatic system, LEC cluster formation was analysed in mice deficient in *Gata2* in the endothelial and haematopoietic cell compartments [*Tie2-Cre:Gata2*$^{flox/flox}$ embryos (*Gata2*$^{\Delta EC}$)] (Kazenwadel et al., 2015). GATA2 is one of the earliest markers of haemogenic endothelium and is essential for haematopoietic development (Gao et al., 2013; Tsai et al., 1994; de Pater et al., 2013). We first validated this model by assessing the development of haematopoietic clusters from haemogenic endothelium in the aorta-gonad-mesonephros (AGM) region of 10.5 dpc wild-type and *Gata2*$^{\Delta EC}$ embryos. Whereas haematopoietic progenitor cells were observed budding from the wall of the dorsal aorta in all littermate control embryos analysed, these cells were depleted in *Gata2*-deficient embryos (Fig. S4C). We next analysed the presence of LEC clusters in the midline region of *Gata2*$^{\Delta EC}$ skin at 13.5 dpc by whole-mount immunostaining (Fig. 3B). Although loss of *Gata2* function in endothelial and haematopoietic lineages resulted in profound defects in lymphatic vascular development, as we previously reported (Kazenwadel et al., 2015), isolated PROX1-positive cells were observed in the dermal capillary plexus of *Gata2*$^{\Delta EC}$ embryos, together with numerous PROX1-positive LEC clusters (Fig. 3B). In fact, the number of LEC clusters documented in *Gata2*$^{\Delta EC}$ embryos was elevated compared with control littermates (Fig. 3B), likely reflecting a much more immature lymphatic network as a result of defective lymphangiogenesis in these mutant mice. These data further demonstrate that haemogenic endothelium is not a progenitor source responsible for the development of dermal LEC clusters. Taken together, our data provide strong evidence to support the concept that, similar to most dermal LECs, dermal LEC clusters are solely of blood vascular endothelial origin.

Local LEC progenitor specification from the dermal blood vascular capillary plexus

The induction of *Prox1* expression in the CVs at ∼9.5 dpc is the earliest LEC specification event in the mouse embryo, and this source of progenitors gives rise to most embryonic LECs (Srinivasan et al., 2007; Wigle and Oliver, 1999). To investigate whether there is a local induction of *Prox1* expression in a subpopulation of dermal capillary endothelial cells, we analysed the embryonic skin of BAC transgenic *Prox1-GFP* embryos (Choi et al., 2011). We observed some ECs scattered throughout the blood capillary plexus that expressed low levels of GFP (Fig. S5A, arrows), suggesting that isolated cells throughout the plexus have

Development (2018) 145, dev160184. doi:10.1242/dev.160184

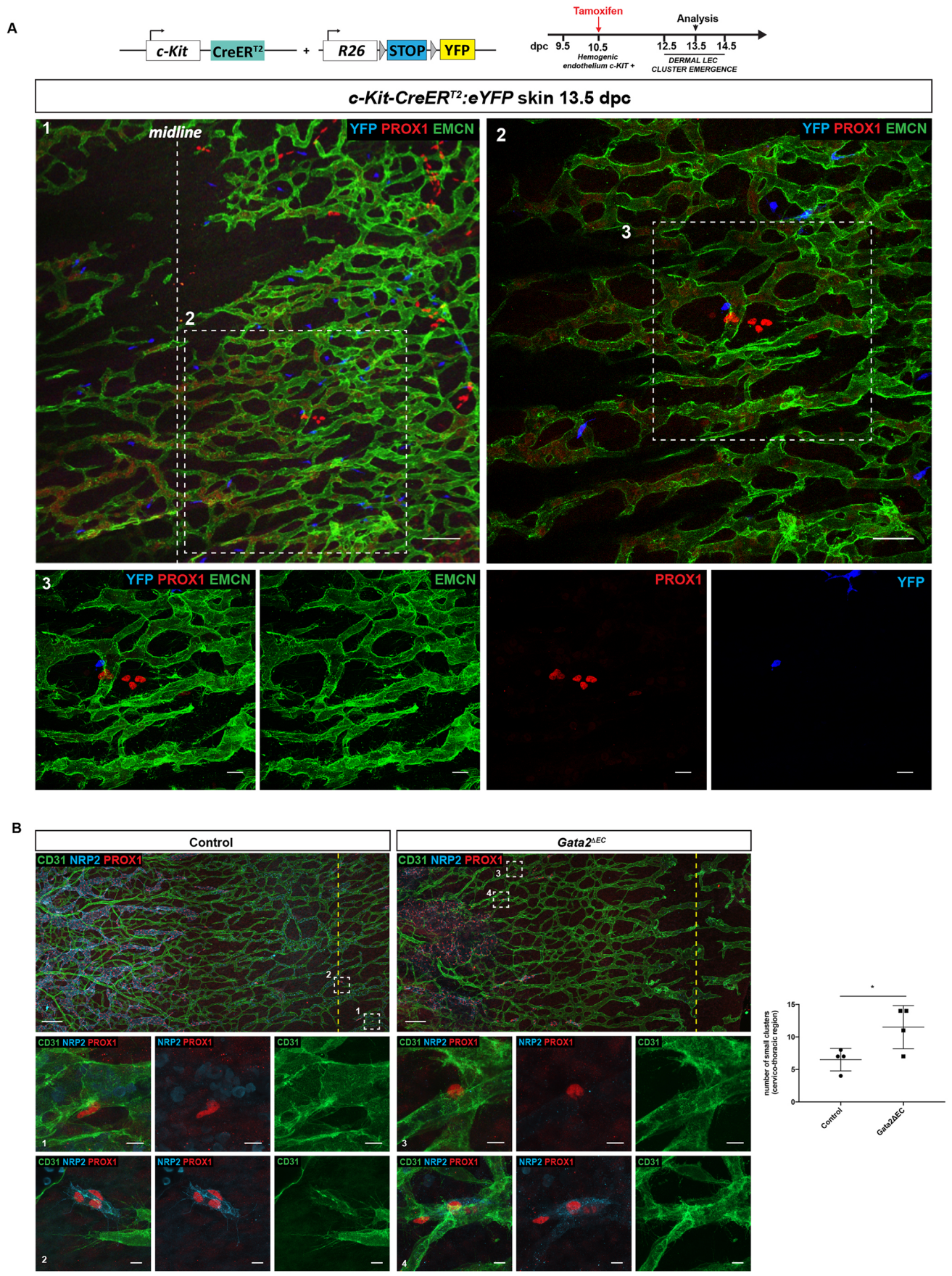

Fig. 3. See next page for legend.

Development (2018) 145, dev160184. doi:10.1242/dev.160184

Fig. 3. LEC clusters do not originate from haemogenic endothelium. (A) Whole-mount immunostaining of *c-Kit-CreERT2:eYFP* skins at 13.5 dpc for EMCN (green), PROX1 (red) and YFP (blue). In this experiment a single dose of tamoxifen was injected at 10.5 dpc (see schematic of the *c-Kit-CreERT2* transgene, *R26R-eYFP* construct and tamoxifen administration schedule above). Scale bars: panel 1 (100 µm); panel 2 (50 µm); panel 3 (20 µm). (B) Whole-mount immunostaining of E13.5 skins from control (left) and *Gata2*$^{\Delta EC}$ (right) embryos labelled with PROX1 (red), CD31 (green) and NRP2 (blue) reveal that LEC clusters develop in the absence of haemogenic endothelium. Boxed regions in top panels are shown at higher magnification in bottom panels. Boxed regions 1 and 3 show single PROX1-positive/NRP2-negative LECs that are associated with the capillary walls and boxed regions 2 and 4 show examples of LEC clusters (expressing much higher levels of NRP2) that have exited the capillary plexus. Dashed yellow line represents dorsal midline. Scale bars: top panels (150 µm), bottom panels (10 µm). Graph shows quantification of LEC clusters in control and *Gata2*$^{\Delta EC}$ skin at 13.5 dpc. Control=4 and *Gata2*$^{\Delta EC}$=4, across 3 litters. Error bars represent s.e.m. **P*<0.05 (unpaired *t*-test).

the potential to turn on *Prox1* transcription. Interestingly, only a subset of these cells exhibited detectable endogenous PROX1 protein (Fig. S5A, arrowhead), suggesting either that *Prox1* levels are post-transcriptionally regulated (Kazenwadel et al., 2010) or, alternatively, that protein levels in these cells were below the threshold detectable by immunostaining. A similar pattern of expression was observed using *Prox1-lacZ* knock-in mice, in which the *lacZ* cassette is inserted into the endogenous *Prox1* locus (Wigle and Oliver, 1999). Isolated β-gal-positive, PROX1-negative cells were found in the endomucin-positive blood capillary plexus, providing further evidence of the capacity of this plexus to activate endogenous *Prox1* transcription (Fig. S5B).

In order to confirm that the dermal blood vascular plexus harbours a source of PROX1-positive LEC progenitors, we used *Prox1-CreERT2:tdTomato* mice and induced Cre recombination by a single pulse of 4-hydroxytamoxifen at 12.5 dpc, the time of LEC cluster emergence in the skin and one that coincides with the downregulation of *Prox1* expression in the jugular veins (former CVs). Skin samples were analysed for tdTomato expression at 13.5 dpc, in order to assess the early events preceding LEC exit from the blood vessels. tdTomato was observed in blood vascular endothelial cells that also expressed endomucin (Fig. 4A) (two out of nine skins analysed), suggesting that *Prox1* transcription is induced in the dermal blood vasculature just prior to the time of LEC cluster generation. To verify that the presence of tdTomato protein was dependent on *Prox1* gene activation upon tamoxifen treatment, we investigated tdTomato levels in skin from embryos that were not exposed to the drug. No tdTomato-positive cells were observed in these skin samples, demonstrating the specificity of Cre recombinase in this model system (nine skins analysed from three independent litters) (Fig. S5C).

Characterisation of both sprouting lymphatic vessels and isolated LEC clusters demonstrated that neither of these populations expresses detectable levels of endomucin (Fig. S6), whereas prominent endomucin staining was observed in the dermal capillary plexus. Immunostaining of *Tie2-Cre:tdTomato* and *Prox1-GFP* skin at 13.5 dpc revealed the presence of cells positive for both PROX1 and endomucin within the capillary bed (Fig. S6). We further confirmed the location of PROX1-positive cells within the inner lining of the capillary wall by analysing high-resolution orthogonal projections of our images. These data confirm that PROX1-positive cells are present in endothelial cells that face the lumen of the capillary plexus at 13.5 dpc (Fig. 4B).

Recent work performed in zebrafish proposed that LEC fate acquisition involves a cell division event in which one daughter cell within the posterior CV upregulates *prox1* expression to establish para-chordal lymphatic vessels, whereas the other cell downregulates *prox1* expression and remains within the wall of the vein (Koltowska et al., 2015). In order to assess whether this mechanism is conserved in mice, we employed the *Prox1-CreERT2:tdTomato* reporter line to investigate whether cell division precedes the exit of LEC progenitors from the dermal capillary plexus. Cre recombinase was activated by the administration of 4-hydroxytamoxifen at 12.5 dpc and skins were analysed at 13.5 dpc. In the case that cell division precedes LEC exit from the capillary wall, tdTomato should be expressed by both mother and daughter cells, whereas PROX1 protein should be restricted to the daughter cell. No tdTomato-positive endothelial cells were observed in any capillary endothelial cells located immediately adjacent to PROX1-positive LEC clusters (ten clusters from six skins) (Fig. 4C). Together, these experiments indicate that LEC clusters in the skin originate from local capillary endothelial cells that turn on endogenous *Prox1* expression without the requirement of an intermediate cell division event.

A local exit from the dermal blood capillary plexus

To investigate the cellular events that underpin the birth of individual LEC clusters, we performed high-resolution imaging of whole-mount immunostained skin from the cervico-thoracic region at 13.5 dpc. At this stage of development, a small number of PROX1-positive clusters, comprising a few cells and characterised by a low level of NRP2 expression, appeared to be connected to the endomucin-positive blood vascular capillary network (Fig. 5A, Movies 1 and 2). Further evidence that LEC clusters emerge from the capillary plexus was provided by many instances in which emerging PROX1-positive cells were observed to share a continuous lumen with blood vessels (Fig. 5A,B, Movies 1 and 2). As a result, circulating blood cells were often found to be engulfed within PROX1-positive LEC clusters (Fig. 5, Movies 1 and 2). The molecular identity of cells encapsulated in LEC clusters was confirmed using an erythrocyte-specific antibody (TER119; also known as LY76) (Fig. 5C). Together, these data demonstrate that dermal LEC clusters physically separate from the endomucin-positive capillary plexus as distinct cellular modalities, either as a single progenitor or as a grouping of a few cells.

The dermal capillary plexus matures by progressively taking on an arterial or venous identity between 12.5 and 16.5 dpc (Mukouyama et al., 2002; Li and Mukouyama, 2013). This biological process is concurrent with LEC cluster formation. Molecular characterisation of the capillary plexus at 13.5 dpc revealed that in the embryonic midline region, capillary endothelial cells were positive for both arterial [SOX17, connexin 40 (CX40; GJA5) and neuropilin 1 (NRP1)] and venous (endomucin) markers (Fig. S7). The expression of arterial markers was lost from the capillary bed from 14.5 dpc onwards. Overall, these experiments demonstrate that arterial and venous markers are not yet restricted at the time of LEC cluster emergence, further supporting the idea that LEC clusters are derived from relatively undifferentiated endothelial cells that retain a level of plasticity (Mukouyama et al., 2002; Li and Mukouyama, 2013).

Emergence of LEC progenitors is dependent on *Ccbe1* and regulated by VEGFC

CCBE1 and VEGFC/VEGFR3 signalling are essential molecular cues required for the sprouting and migration of LEC progenitors from the cardinal and intersomitic veins (Karkkainen et al., 2004; Bos et al., 2011; Hägerling et al., 2013). Genetic ablation of *Ccbe1*

Development (2018) 145, dev160184. doi:10.1242/dev.160184

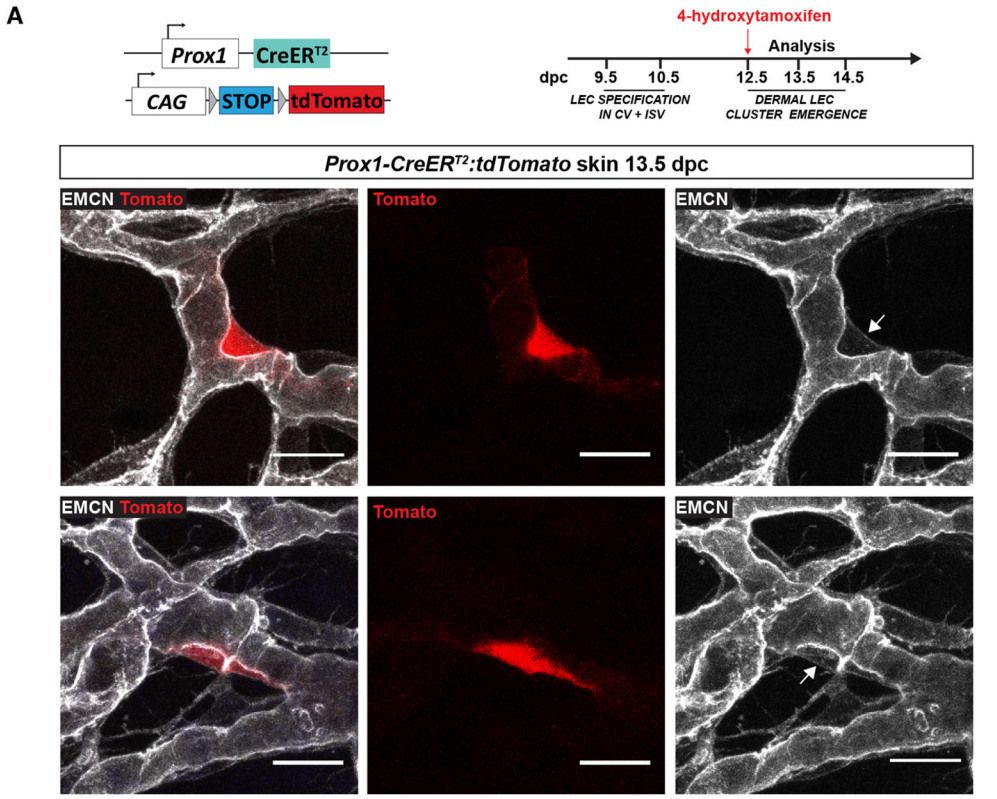

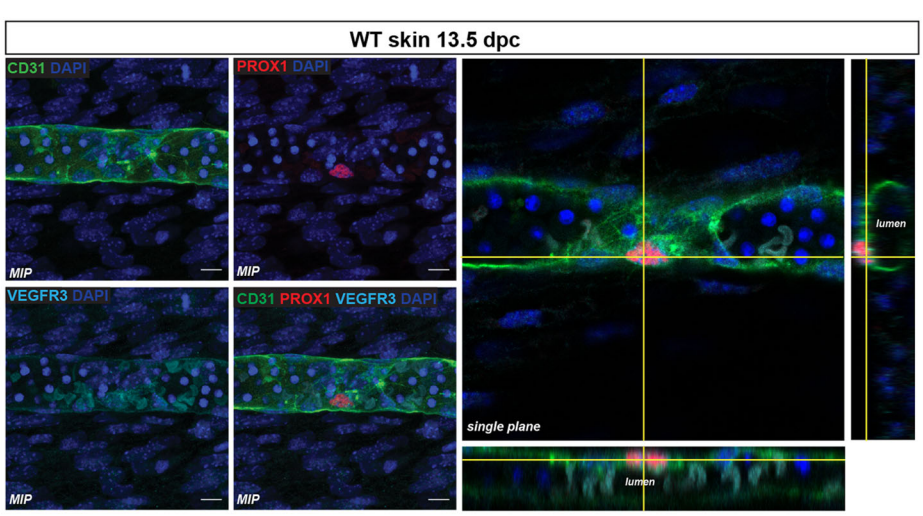

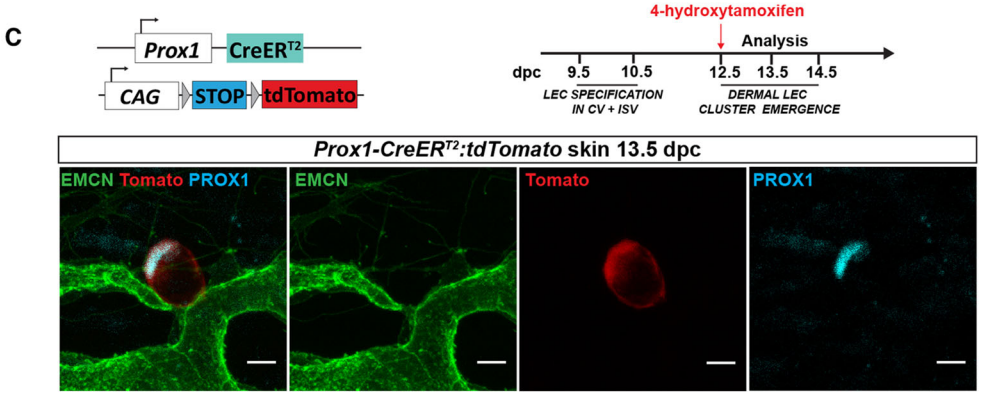

Fig. 4. Dermal LEC progenitors are specified within the blood vascular capillary plexus. (A) Whole-mount immunostaining of embryonic skin at 13.5 dpc for EMCN (grey). tdTomato expression is detected in endomucin-positive cells demonstrating activation of *Prox1* gene transcription. Arrows indicate PROX1-positive/endomucin-positive cells. Scale bars: 20 µm. (B) Whole-mount immunostaining of wild-type (WT) embryonic skin at 13.5 dpc for PROX1 (red) and CD31 (green), VEGFR3 (light blue) and DAPI (dark blue). Left: Maximum intensity projections (MIP). Right: Orthogonal projection from the *z*-stack with *xz* and *yz* views showing PROX1-positive cell in the endothelial wall lining. Scale bars: 10 µm. (C) Whole-mount immunostaining of skin for PROX1 (blue) and EMCN (green) from *Prox1-CreERT2:tdTomato* embryo at 13.5 dpc. Cre recombinase was activated by a single injection of 4-hydroxytamoxifen at 12.5 dpc. Scale bars: 10 µm. Schematics of the *Prox1-CreERT2:tdTomato* construct and 4-hydroxytamoxifen injection schedules are shown in A and C.

Development (2018) 145, dev160184. doi:10.1242/dev.160184

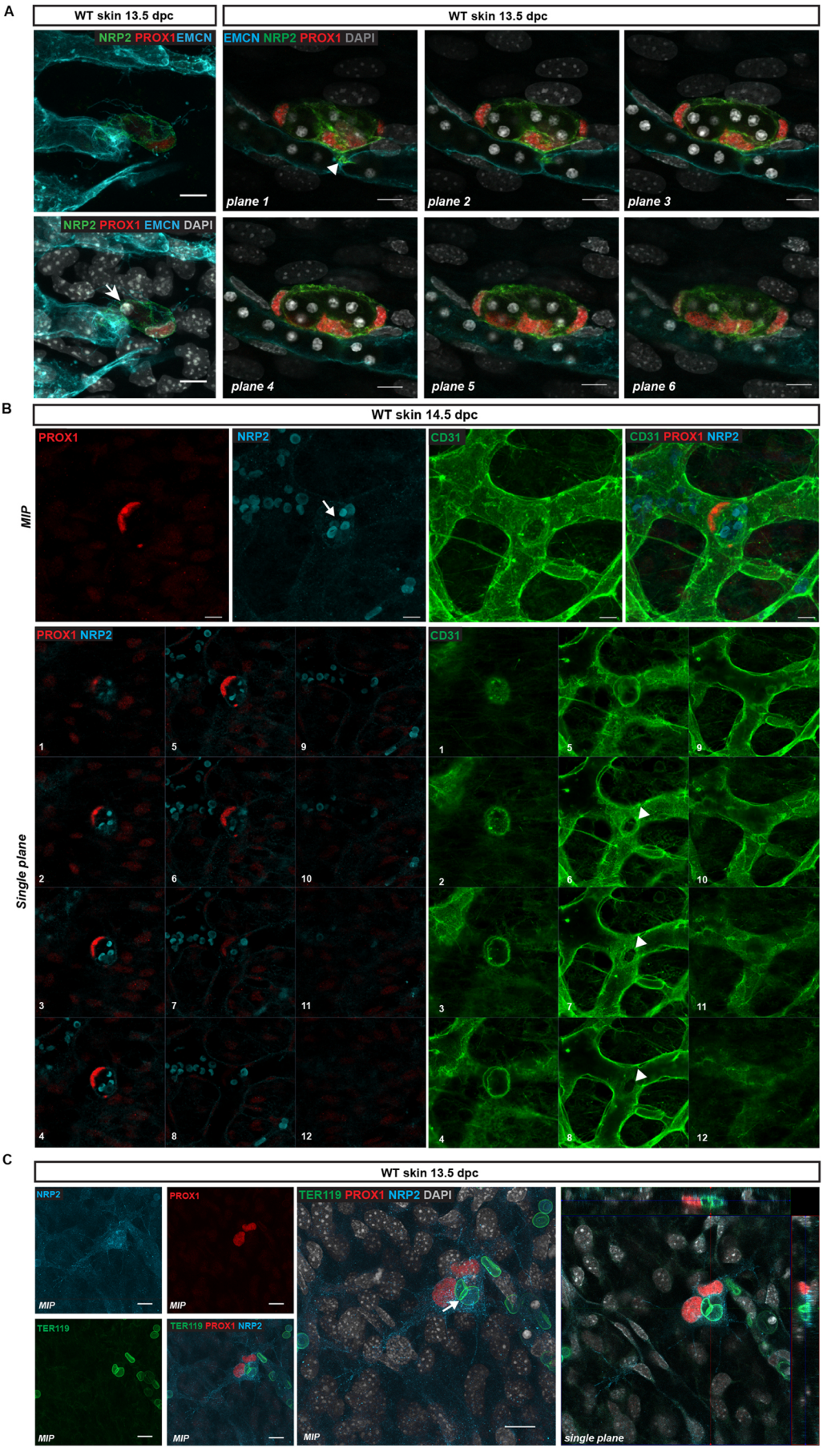

Fig. 5. LEC clusters bud from the dermal blood vascular capillary plexus. (A) Left: Whole-mount immunostaining of wild-type (WT) embryonic skin at 13.5 dpc. LEC progenitors stained with NRP2 (green) and PROX1 (red) delaminate from the endomucin-positive capillary plexus (blue). Staining of the nuclei with DAPI reveals that this event is associated with the encapsulation of red blood cells (arrow). Right: Whole-mount immunostaining of WT embryonic skin at 13.5 dpc for EMCN (blue), NRP2 (green) and PROX1 (red) showing multiple PROX1-positive LEC progenitors undergoing cell extrusion from the capillary plexus. Each image corresponds to a single plane through a maximum intensity projection (MIP). Arrowhead indicates the connection point between the LEC cluster and the blood vascular plexus. Red blood cells, visualised by DAPI staining, are encapsulated by LECs. (B) Whole-mount immunostaining of WT embryonic skin at 14.5 dpc for PROX1 (red), CD31 (green) and NRP2 (blue) showing a PROX1-positive lymphatic cluster emerging from the blood vascular plexus, encapsulating multiple red blood cells (arrow; highlighted by NRP2). Top panels show MIPs, bottom panels show individual single planes (1-12) through the MIP showing the connection between the lymphatic cluster and blood vascular plexus (arrowheads). Plane 1 depicts the top of the cluster, and planes 6-8 show the connection point with the blood vasculature. (C) Whole-mount immunostaining of WT embryonic skin at 13.5 dpc. LEC cluster stained with NRP2 (blue) and PROX1 (red) showing encapsulation of red blood cells (stained with TER119 antibody, green). Arrow indicates red blood cell present within the LEC cluster. Left panels show MIPs, right panel shows an orthogonal projection from the *z*-stack with *xz* and *yz* views showing the encapsulated red blood cell. Scale bars: 10 µm.

Development (2018) 145, dev160184. doi:10.1242/dev.160184

results in the loss of definitive lymphatic structures in both zebrafish and mice (Bos et al., 2011; Hogan et al., 2009) due to the failure of PROX1-positive cells to exit and migrate away from the CVs (Hägerling et al., 2013). To confirm that LEC progenitors are specified locally in the dermal capillary plexus and to investigate whether their exit is dependent on *Ccbe1*, we took advantage of *Ccbe1*-deficient mice (Bos et al., 2011). As previously reported, no lymphatic vessels were observed in the skin of *Ccbe1* null embryos at 13.5 dpc and, likewise, no LEC clusters were present (Fig. 6A). By contrast, isolated PROX1-positive LEC progenitors were visible within the vessel walls of endomucin-positive vessels of *Ccbe1*-deficient embryos (Fig. 6A). No significant difference in the number of PROX1-positive cells in the capillary plexus was observed between *Ccbe1* null embryos and their control littermates (Fig. 6A). These data reveal that the exit of PROX1-positive cells from the capillary plexus is dependent on *Ccbe1*, as is the case for the exit of PROX1-positive LEC progenitors from the CVs and ISVs. In a complementary approach, we investigated whether gain of VEGFC function in endothelial cells could influence the induction of PROX1-positive cells within the capillary plexus. *Tie2-Cre* was used to activate *Vegfc* expression in blood vascular endothelial cells. Analysis of *Tie2Cre;VegfcGOF* embryonic skin at 12.5 dpc revealed a dramatic increase in the number of PROX1-positive cells in the endomucin-positive plexus (Fig. 6B). The dependence of LEC cluster development on *Prox1* was investigated by analysing the number of LEC clusters in the skin of *Prox1* heterozygous embryos; $Prox1^{+/lacZ}$ skin harboured a significantly decreased number of LEC clusters compared with littermate controls (Fig. S5D). Together, these powerful genetic gain- and loss-of-function approaches provide further evidence that LEC cluster formation involves a local specification event that occurs within the primitive capillary plexus and is regulated by *Ccbe1*, *Vegfc* and *Prox1*.

DISCUSSION

Here, we demonstrate that the dermal blood vascular capillary plexus provides an additional source of LECs employed during construction of the lymphatic vasculature in embryonic mouse skin. This finding reveals that LEC specification from an endothelial origin is not restricted to the CVs and ISVs during early embryogenesis, but is an event that proceeds in the dermal capillary bed also at later stages of development. In particular, we identify a time window between 12.5 and 15.5 dpc when isolated endothelial cells in the midline region of the dermal capillary plexus turn on *Prox1* and detach from the capillary bed via a budding mechanism, acquiring and upregulating the expression of LEC markers including podoplanin, NRP2 and VEGFR3 upon their exit. These cells subsequently proliferate to generate LEC clusters and sprout to meet up with the centrifugally sprouting lymphatic vascular plexus, forming an interconnected lymphatic vessel network. These results argue that during mammalian embryonic lymphangiogenesis, the same genes and mechanisms participating in the formation of the initial PROX1-positive LEC progenitors in the CVs are used again later on by other vascular beds (i.e. budding of PROX1-positive progenitors that acquire additional LEC markers upon their exit from blood vessels and regulation of this process by *Vegfc* and *Ccbe1*). We propose a dual mechanism of lymphangiogenesis in the skin that relies on a combination of centrifugal sprouting and local budding and differentiation (Fig. 7).

Isolated LEC clusters have been previously described in embryonic mouse skin (Hirashima et al., 2008; James et al., 2013; Martinez-Corral et al., 2015), but their cellular origin remained elusive. Recent work suggested that small groups of LECs in the lumbar and midline regions of the mouse embryo are derived from a non-venous origin (Martinez-Corral et al., 2015). However, our results demonstrate that LEC clusters in the cervico-dorsal region are derived from the local immature capillary plexus, and that clusters in the lumbar region might also have a similar origin. Because lymphatic vascular development progresses in an antero-posterior manner (Sabin, 1902), it is likely that processes that occur first in the cervical region are recapitulated at a later stage in the lumbar and sacral midline regions. Using the *Tie2-Cre:tdTomato* line, we found that LEC clusters in the dorsal lumbar midline region were also Tomato positive, suggesting that they arise from the same cellular origin as do cervical clusters. The discrepancy between the results generated in our study and those of Martinez-Corral et al. could reflect previously described variability in *Tie2-Cre*-mediated recombination, which can be prominent even within the same litter of embryos (our data; Heffner et al., 2012).

Previous analysis of *Ccbe1*-deficient mice revealed a potential second venous source of LEC progenitor cells in the mouse embryo at 11.5 dpc: the superficial venous plexus (Hägerling et al., 2013). Our data reveal that, intriguingly, the capillary plexus in the dermis, which generates LEC progenitors, exhibits a mixed endothelial cell identity at 13.5 dpc, co-expressing both arterial and venous markers. These data suggest that vascular beds other than fully differentiated veins have the potential to give rise to LECs. This finding is congruent with recent reports in zebrafish, in which facial lymphatic vessels were suggested to arise from various blood vessel origins (Okuda et al., 2012).

Using genetic lineage-tracing approaches combined with mutant mouse models and analysis of endogenous gene expression, we were able to exclude the haemogenic endothelium as a source of LEC progenitors in embryonic mouse skin. The strategy of tamoxifen-induced *c-Kit-CreERT2* activity at 10.5 dpc allowed us to assess the involvement of both intra- and extra-embryonic haemogenic endothelium as a potential source of LEC progenitors. The failure to detect any c-KIT lineage-derived LECs revealed that c-KIT-positive haemogenic endothelium is not a source of LEC progenitors that contributes to lymphangiogenesis in the skin, in contrast to the scenario in mesenteric lymphatic development. In a parallel approach, analysis of mice deficient in *Gata2* allowed us to target *Tie2*-positive haemogenic endothelium from the YS that could potentially have been missed using the *c-Kit-CreERT2* lineage-tracing approach employed. The presence of LEC clusters in *Gata2*-deficient embryos strongly suggests that neither the YS nor intra-embryonic haemogenic endothelium is involved in dermal lymphatic vessel formation. Our data diverge from previous observations in other organs, which demonstrated that haemogenic endothelium has the capacity to provide a population of LECs employed during construction of the mesenteric and cardiac lymphatic vasculature (Klotz et al., 2015; Stanczuk et al., 2015). The differences in progenitor cell pools that contribute to lymphangiogenesis suggest that lymphatic vessel network assembly is likely to rely on organ-specific physiological requirements.

Although genetic lineage tracing is a powerful tool, limitations such as incomplete Cre-mediated recombination and aberrant, ectopic Cre activity have been reported (Heffner et al., 2012; Ulvmar et al., 2016). In order to gain complementary information on the cellular origin of LEC clusters and also to investigate precisely the cellular behaviour underlying cluster formation, we used high-resolution confocal microscopy to analyse endogenous protein expression. Together, these approaches enabled us to describe a budding mechanism by which LEC progenitors physically emerge

Development (2018) 145, dev160184. doi:10.1242/dev.160184

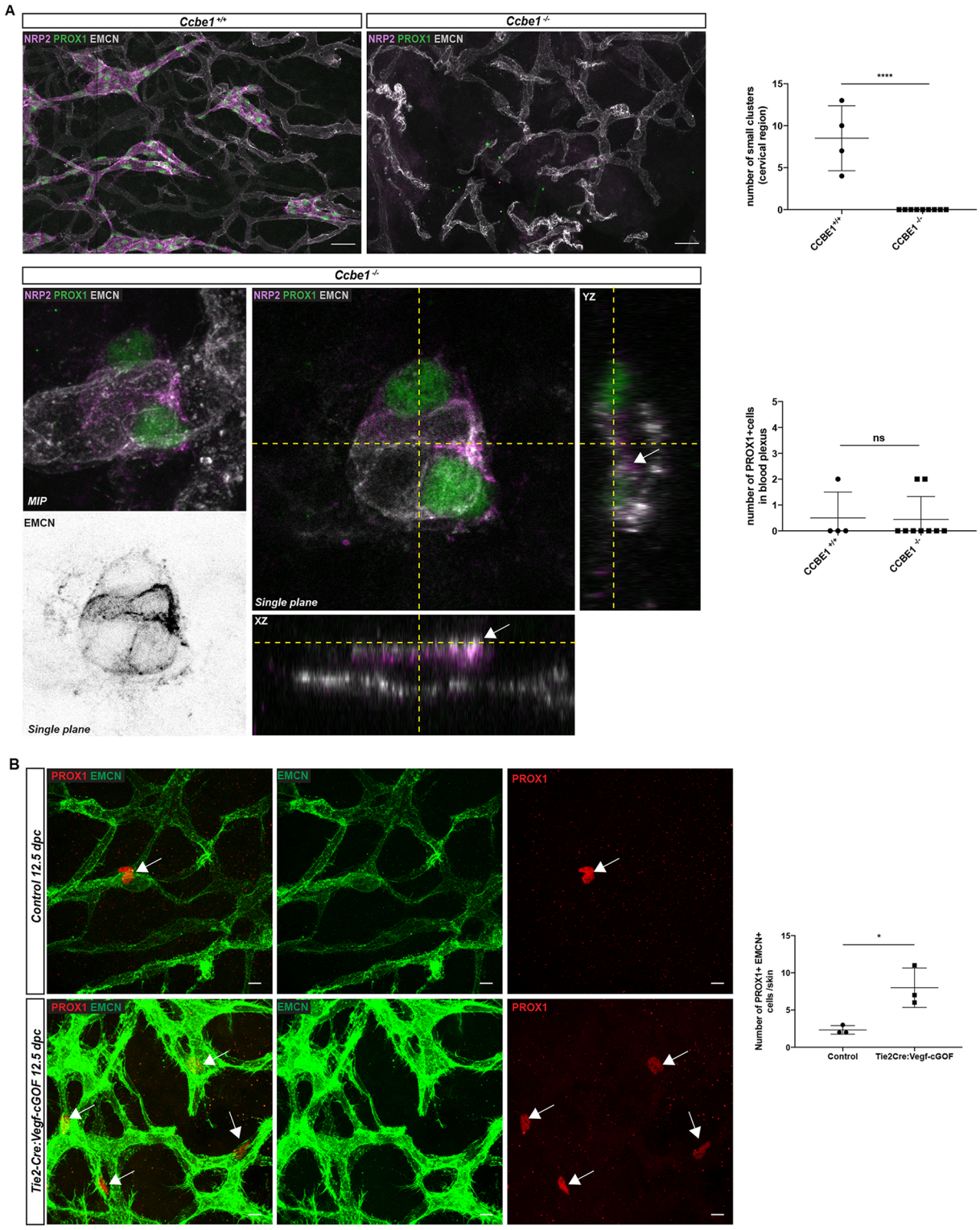

Fig. 6. Exit of LEC progenitors from the dermal capillary plexus is dependent on CCBE1/VEGFC/VEGFR3 signalling. (A) Whole-mount immunostaining of *Ccbe1*$^{+/+}$ and *Ccbe1*$^{-/-}$ embryonic skin at 13.5 dpc for PROX1 (green), NRP2 (purple) and EMCN (grey). Top: In contrast to littermate control embryos, the dermal lymphatic network is absent in *Ccbe1*$^{-/-}$ embryos. Scale bars: 50 µm. Bottom: Maximum intensity projection (MIP) and orthogonal projection from the *z*-stack with *xz* and *yz* views showing isolated PROX1-positive cells within the endomucin-positive capillary plexus of *Ccbe1*$^{-/-}$ skin. Greyscale image shows a detection channel for EMCN (endomucin) staining only. This single plane signal is obtained from the triple staining (NRP2, PROX1, EMCN) shown for the LEC cluster of a Ccbe1-null embryo (centre panel). Top graph represents the number of small LEC clusters (maximum four cells per cluster) in the cervico-thoracic region in *Ccbe1*$^{+/+}$ and *Ccbe1*$^{-/-}$ embryonic skin. *Ccbe1*$^{+/+}$, *n*= 4 skins; *Ccbe1*$^{-/-}$, *n*=9 skins. Bottom graph represents the number of PROX1-positive/endomucin-positive cells in the endothelial lining in *Ccbe1*$^{+/+}$ and *Ccbe1*$^{-/-}$ embryonic skin. Error bars represent s.e.m. ****P<0.0001; ns, not significant (unpaired *t*-test). (B) Whole-mount immunostaining of control and *Tie2-Cre:VegfcGOF* embryonic skin at 12.5 dpc for PROX1 (red) and EMCN (green). Arrows indicate PROX1-positive/endomucin-positive LEC progenitors. Graph shows the quantification of the number of PROX1-positive cells in the EMCN-positive plexus comparing control transgenic and Tie2-Cre VEGFC GOF. Error bars represent s.e.m. *P<0.05 (unpaired *t*-test; *n*=3).

Development (2018) 145, dev160184. doi:10.1242/dev.160184

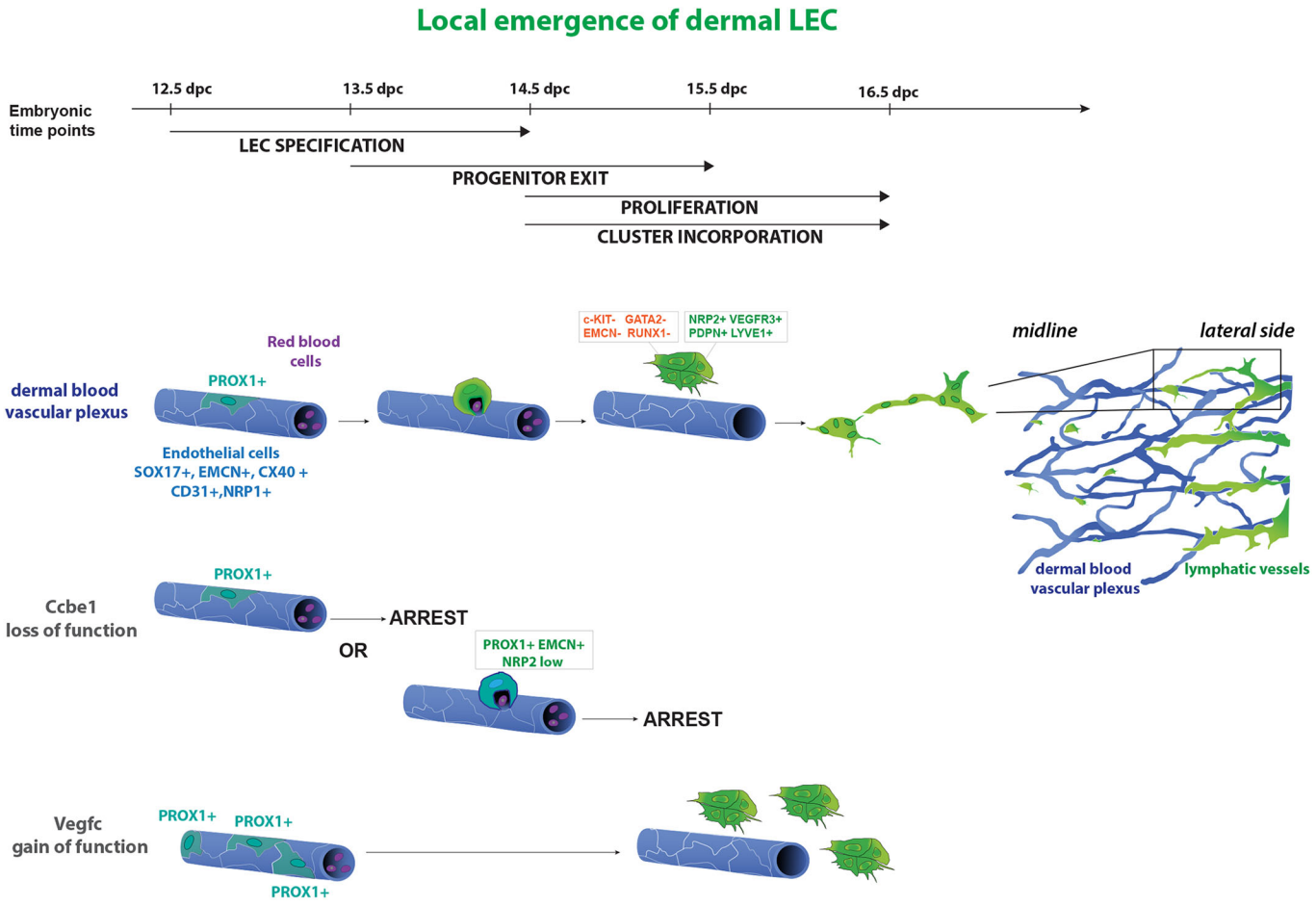

Fig. 7. A model of dermal lymphangiogenesis. Schematic of local LEC progenitor emergence from the dermal blood vascular plexus. From 12.5 dpc a subset of endothelial cells in the dermal blood vascular capillary plexus (blue) turn on PROX1 expression. These cells subsequently exit the plexus, acquire PDPN and start to upregulate lymphatic markers including NRP2, VEGFR3 and LYVE1. Following exit from the capillary plexus, LECs proliferate and, ultimately, connect to the main lymphatic vessel network (green) to form a functional, interconnected network. In *Ccbe1*$^{-/-}$ embryos, LEC progenitors remain embedded within the vessel wall of the capillary plexus. *Vegfc* gain of function in blood vessel endothelial cells results in a dramatic increase in the number of PROX1-positive cells in the endomucin-positive plexus.

and detach from the blood capillary plexus. Our observations documenting LECs encapsulating red blood cells provided further evidence of the existence of transient connections between emerging LEC clusters and the capillary plexus. Similar structures have been previously reported during the emergence of the initial lymphatic vascular plexus from the CV (François et al., 2012). It remains to be determined whether the interaction of circulating blood components with endothelial cells is a key determining factor in the physical separation of LECs from blood vascular endothelium. It is known that platelets play an active role during the separation of blood and lymphatic vascular networks by providing a seal that prevents initial bleeding into nascent lymphatic structures (Bertozzi et al., 2010; Carramolino et al., 2010; Uhrin et al., 2010). Whether circulating blood moieties also provide directive sprouting signals remains to be determined.

The molecular changes involved in the emergence of LEC progenitors from the dermal capillary plexus appear to be shared with those that feature during LEC progenitor exit from the CVs and ISVs at an earlier stage of development. As LEC progenitors physically separate from the blood capillary plexus from which they originate, LEC-specific markers, including PDPN, are acquired. Similarly to the VEGFC-driven exit of LECs from the CV, LEC exit from the dermal capillary plexus is dependent on *Ccbe1* and regulated by VEGFC. The molecular driver that induces *Prox1* expression in a subset of endothelial cells in the capillary plexus remains to be determined. The transcription factors SOX18 and COUP-TFII (NR2F2) have been shown to activate *Prox1* transcription directly in a subpopulation of venous ECs (François et al., 2008; Srinivasan et al., 2010), but their inductive cues remain elusive. It is possible that *Prox1* expression might be induced in response to the tissue-restricted expression of growth factors, including VEGFC, although at present the identity of cells providing such cues is not established. Previous studies in zebrafish suggested that Vegfc signalling could be directly involved in the induction of *Prox1* expression (Koltowska et al., 2015). Our data provide further support for an important role for VEGFC signalling in the specification and/or expansion of the LEC progenitor population.

Taken together, our data demonstrate that LEC specification occurs not only within the embryonic cardinal and intersomitic veins during development, but also within a subpopulation of relatively undifferentiated endothelial cells of the dermal blood vascular capillary plexus. We propose that these differential sources of LECs allow the dermal lymphatic vascular network to be constructed more rapidly and efficiently than a mechanism relying solely on sprouting and migration of LEC from the flanks to the

Development (2018) 145, dev160184. doi:10.1242/dev.160184

midline. Whether the LECs generated from the dermal capillary bed have a unique function within the lymphatic vasculature and the magnitude to which the selective disruption of this source of LEC progenitors would impact the process of lymphangiogenesis in the skin remain open questions to be addressed in future work. Our findings also raise the question of whether capillary beds in other tissues might harbour a source of LECs employed during genesis of the lymphatic vasculature in a range of organs, together with the possibility that these vascular beds might be a source of LEC progenitors recruited during pathological lymphangiogenesis.

MATERIALS AND METHODS

Mice

The following mice used in this study have been described previously: *Sox18-CreERT2* (McMahon et al., 2008), *Cdh5-CreERT2* (Wang et al., 2010), *Tie2-Cre* (Kisanuki et al., 2001), *B6.Cg-Gt(ROSA)26Sor*$^{tm9(CAG-tdTomato)Hze}$*/J* (Madisen et al., 2010), *c-Kit-CreERT2* (Klein et al., 2013), *R26R-eYFP* (Srinivas et al., 2001), *Gata2*$^{flox/flox}$ (Haugas et al., 2010), *Ccbe1*$^{lacZ/lacZ}$ (Bos et al., 2011), *Prox1-CreERT2* (Srinivasan et al., 2007), *Tie2-GFP* (Motoike et al., 2000), *Lyve1GFP-Cre* (Pham et al., 2010). To generate the conditional *Vegfc* gain-of-function (*VegfcGOF*) mouse model, the full-length cDNA of mouse *Vegfc* with a V5 tag was inserted into the first intron of the *Eif1a* locus. *Vegfc* expression was prevented by a floxed neomycin-triple poly(A) cassette preceding *Vegfc*, and was induced upon Cre-mediated excision of this sequence (Fig. S8). All experiments using mice were approved and conducted in accordance with the SA Pathology/CALHN Animal Ethics Committee, University of Queensland Animal Ethics Committee, Northwestern University Institutional Animal Care and Use Committee and Australian National Health and Medical Research Council (NHMRC) guidelines.

Tamoxifen and 4-hydroxytamoxifen treatment

For lineage-tracing experiments, pregnant mice received a single intraperitoneal injection of 1 mg of tamoxifen or 4-hydroxytamoxifen (Sigma-Aldrich, H6278-50MG). Briefly, 100 mg (tamoxifen) or 50 mg (4-hydroxytamoxifen) was reconstituted in 10% (v/v) ethanol and 90% (v/v) peanut oil.

Antibodies

Goat anti-PROX1 (1:200, AF2727, R&D Systems), rabbit anti-PROX1 (1:200, 11-002, AngioBio), rabbit anti-PROX1 (1:200, ab101851, Abcam), rat anti-mouse CD31 (1:200, 553370, BD Pharmingen), hamster anti-podoplanin (1:1000, 8.1.1, Developmental Studies Hybridoma Bank), goat anti-NRP2 (1:200, AF567, R&D Systems), XP rabbit anti-NRP2 (1:500, 3366, Cell Signaling), goat anti-NRP1 (1:300, AF566, R&D Systems), goat anti-VECAD (1:200, sc-6458, Santa Cruz Biotechnology), rabbit anti-GATA2 (1:1000, NBP1-82581, Novus Biologicals), rat anti-endomucin (EMCN) (1:400, sc-53941, Santa Cruz Biotechnology), rat anti-CD45 (PTPRC) (1:250, 553076, BD Pharmingen), anti-CD117 (c-Kit) (1:250, 553354, eBioscience), goat anti-c-KIT (1:100, AF1356, R&D Systems), rat anti-CD34 (1:250, 14-0341, eBioscience), rabbit anti-RUNX1/AML1 +RUNX3+RUNX2 (1:500, ab92336, Abcam), goat anti-VEGFR3 (1:500, AF743, R&D Systems), goat anti-SOX17 (1:200, AF1924, R&D Systems), rat anti-TER119 (1:200, 14-5921-82, Thermo Fisher Scientific), chicken anti-GFP (1:200, ab13970, Abcam), chicken anti-β-gal (1:500, ab9361, Abcam) and rabbit anti-connexin 40 (1:200, CX40A, Alpha Diagnostic International) antibodies were all used for immunostaining. Alexa Fluor fluorochrome-conjugated antibodies were used for detection at 1:200 (Invitrogen): Alexa 488 donkey anti-goat A-11055, Alexa 546 goat anti-rabbit A-11010, Alexa 647 goat anti-rabbit A-31573, Alexa 647 goat anti-rat A-21247 and Alexa 488 goat anti-rat A-21208.

Whole-mount immunostaining

For whole-mount immunostaining of embryonic skin, embryos were fixed in 4% paraformaldehyde (PFA) overnight at 4°C. Skin samples were dissected post-fixation and blocked in PBS containing 10% heat-inactivated horse serum, 100 mM maleic acid, 1% DMSO and 0.1% Triton X-100 for 1 h at 4°C. Following blocking, skin samples were incubated with primary antibodies diluted in blocking solution overnight at 4°C and then washed extensively in PBS containing 0.1% Triton X-100 and 1% DMSO. Skin samples were then incubated with Alexa Fluor-conjugated secondary antibodies overnight at 4°C (or for 4 h at room temperature) and washed as outlined above. Samples were mounted in 80% glycerol or using DAPI Fluoromount G (ProSciTech).

EdU injection and analysis of proliferation

Proliferating cells were detected using the Click-iT Edu Imaging Kit (Invitrogen). Briefly, 1 mg of EdU was injected intraperitoneally to pregnant mice. After 4 h, mice were humanely killed and embryos were fixed overnight in 4% PFA at 4°C. Embryos were then washed in PBS and skins were dissected and processed for immunostaining as described above. After incubation with secondary antibody, skins were washed extensively in PBS and incubated in the Click-iT reaction cocktail for 1 h at room temperature. Skins were then washed in PBS prior to mounting as described above.

Image acquisition

Images were captured at room temperature using either a Zeiss LSM 710 META BIG or Zeiss LSM 700 confocal microscope with a 10×, 20×, 40× or 63× oil objective. Images were analysed using Zen software (Zeiss) and ImageJ (Abramoff et al., 2004).

Image processing

For Fig. S7B, the noise despeckle function was used for all the images in order to reduce the noise of the signal using ImageJ software.

Acknowledgements

We thank Chris Brown and staff at the SA Pathology Animal Facility for animal husbandry. Transgenic (*Tie2-GFP*) embryonic material was provided by Frank Bos and Jacco van Rheenen (Hubrecht Institute). Imaging at IMB was supported by ACRF microscopy facility. The DSHB Hybridoma Product 8.1.1 (podoplanin) developed by A. G. Farr (University of Washington) was obtained from the Developmental Studies Hybridoma Bank, created by The NICHD of the NIH and maintained at the University of Iowa, Department of Biology, Iowa City, IA, 52242, USA.

Competing interests

The authors declare no competing or financial interests.

Author contributions

Conceptualization: C.P.-T., B.M.H., N.L.H., M.F.; Methodology: C.P.-T.; Validation: C.P.-T., K.L.B.; Formal analysis: C.P.-T., K.L.B.; Investigation: C.P.-T., K.L.B., X.L., W.M., R.S., E.L., F.L.B.; Resources: R.S., E.L., D.S., S.S.-M., G.O.; Writing - original draft: C.P.-T., K.L.B., G.O., N.L.H., M.F.; Writing - review & editing: C.P.-T., K.L.B., X.L., D.S., B.M.H., G.O., N.L.H., M.F.; Visualization: C.P.-T., K.L.B., X.L., G.O., N.L.H., M.F.; Supervision: M.F., B.M.H., N.L.H.; Project administration: N.L.H., M.F.; Funding acquisition: S.S.-M., G.O., N.L.H., M.F.

Funding

This work was supported by grants from the National Health and Medical Research Council (NHMRC) (APP1107643 to M.F. and N.L.H.), Australian Research Council (ARC) (DP150103110 to B.M.H. and N.L.H.) and National Institutes of Health (R01-HL073402 to G.O.). N.L.H. is supported by an ARC Future Fellowship (FT130101254). M.F. is supported by an NHMRC Career Developmental Fellowship (APP1111169). B.M.H. is supported by an NHMRC/National Heart Foundation of Australia Career Development Fellowship (1083811). F.L.B. was supported by Netherlands Cancer Society (KWF Kankerbestrijding) Fellowship 6660. Deposited in PMC for release after 12 months.

Supplementary information

Supplementary information available online at
http://dev.biologists.org/lookup/doi/10.1242/dev.160184.supplemental

References

Abramoff, M. D., Magalhaes, M. P. and Ram, S. J. (2004). Image processing with ImageJ. *Biophoton. Int.* **11**, 7.

Antila, S., Karaman, S., Nurmi, H., Airavaara, M., Voutilainen, M. H., Mathivet, T., Chilov, D., Li, Z., Koppinen, T., Park, J.-H. et al. (2017). Development and plasticity of meningeal lymphatic vessels. *J. Exp. Med.* **214**, 3645-3667.

Bertozzi, C. C., Hess, P. R. and Kahn, M. L. (2010). Platelets: covert regulators of lymphatic development. *Arterioscler. Thromb. Vasc. Biol.* **30**, 2368-2371.
Bos, F. L., Caunt, M., Peterson-Maduro, J., Planas-Paz, L., Kowalski, J., Karpanen, T., van Impel, A., Tong, R., Ernst, J. A., Korving, J. et al. (2011). CCBE1 is essential for mammalian lymphatic vascular development and enhances the lymphangiogenic effect of vascular endothelial growth factor-C in vivo. *Circ. Res.* **109**, 486-491.
Carramolino, L., Fuentes, J., Garcia-Andres, C., Azcoitia, V., Riethmacher, D. and Torres, M. (2010). Platelets play an essential role in separating the blood and lymphatic vasculatures during embryonic angiogenesis. *Circ. Res.* **106**, 1197-1201.
Choi, I., Chung, H. K., Ramu, S., Lee, H. N., Kim, K. E., Lee, S., Yoo, J., Choi, D., Lee, Y. S., Aguilar, B. et al. (2011). Visualization of lymphatic vessels by Prox1-promoter directed GFP reporter in a bacterial artificial chromosome-based transgenic mouse. *Blood* **117**, 362-365.
de Pater, E., Kaimakis, P., Vink, C. S., Yokomizo, T., Yamada-Inagawa, T., van der Linden, R., Kartalaei, P. S., Camper, S. A., Speck, N. and Dzierzak, E. (2013). Gata2 is required for HSC generation and survival. *J. Exp. Med.* **210**, 2843-2850.
François, M., Caprini, A., Hosking, B., Orsenigo, F., Wilhelm, D., Browne, C., Paavonen, K., Karnezis, T., Shayan, R., Downes, M. et al. (2008). Sox18 induces development of the lymphatic vasculature in mice. *Nature* **456**, 643-647.
François, M., Short, K., Secker, G. A., Combes, A., Schwarz, Q., Davidson, T.-L., Smyth, I., Hong, Y.-K., Harvey, N. L. and Koopman, P. (2012). Segmental territories along the cardinal veins generate lymph sacs via a ballooning mechanism during embryonic lymphangiogenesis in mice. *Dev. Biol.* **364**, 89-98.
Gao, X., Johnson, K. D., Chang, Y.-I., Boyer, M. E., Dewey, C. N., Zhang, J. and Bresnick, E. H. (2013). Gata2 cis-element is required for hematopoietic stem cell generation in the mammalian embryo. *J. Exp. Med.* **210**, 2833-2842.
Hägerling, R., Pollmann, C., Andreas, M., Schmidt, C., Nurmi, H., Adams, R. H., Alitalo, K., Andresen, V., Schulte-Merker, S. and Kiefer, F. (2013). A novel multistep mechanism for initial lymphangiogenesis in mouse embryos based on ultramicroscopy. *EMBO J.* **32**, 629-644.
Haugas, M., Lilleväli, K., Hakanen, J. and Salminen, M. (2010). Gata2 is required for the development of inner ear semicircular ducts and the surrounding perilymphatic space. *Dev. Dyn.* **239**, 2452-2469.
Heffner, C. S., Herbert Pratt, C., Babiuk, R. P., Sharma, Y., Rockwood, S. F., Donahue, L. R., Eppig, J. T. and Murray, S. A. (2012). Supporting conditional mouse mutagenesis with a comprehensive cre characterization resource. *Nat. Commun.* **3**, 1218.
Hirashima, M., Sano, K., Morisada, T., Murakami, K., Rossant, J. and Suda, T. (2008). Lymphatic vessel assembly is impaired in Aspp1-deficient mouse embryos. *Dev. Biol.* **316**, 149-159.
Hogan, B. M., Bos, F. L., Bussmann, J., Witte, M., Chi, N. C., Duckers, H. J. and Schulte-Merker, S. (2009). Ccbe1 is required for embryonic lymphangiogenesis and venous sprouting. *Nat. Genet.* **41**, 396-398.
James, J. M., Nalbandian, A. and Mukouyama, Y.-S. (2013). TGFbeta signaling is required for sprouting lymphangiogenesis during lymphatic network development in the skin. *Development* **140**, 3903-3914.
Karkkainen, M. J., Haiko, P., Sainio, K., Partanen, J., Taipale, J., Petrova, T. V., Jeltsch, M., Jackson, D. G., Talikka, M., Rauvala, H. et al. (2004). Vascular endothelial growth factor C is required for sprouting of the first lymphatic vessels from embryonic veins. *Nat. Immunol.* **5**, 74-80.
Kazenwadel, J., Michael, M. Z. and Harvey, N. L. (2010). Prox1 expression is negatively regulated by miR-181 in endothelial cells. *Blood* **116**, 2395-2401.
Kazenwadel, J., Betterman, K. L., Chong, C.-E., Stokes, P. H., Lee, Y. K., Secker, G. A., Agalarov, Y., Demir, C. S., Lawrence, D. M., Sutton, D. L. et al. (2015). GATA2 is required for lymphatic vessel valve development and maintenance. *J. Clin. Invest.* **125**, 2979-2994.
Kisanuki, Y. Y., Hammer, R. E., Miyazaki, J., Williams, S. C., Richardson, J. A. and Yanagisawa, M. (2001). Tie2-Cre transgenic mice: a new model for endothelial cell-lineage analysis in vivo. *Dev. Biol.* **230**, 230-242.
Klein, S., Seidler, B., Kettenberger, A., Sibaev, A., Rohn, M., Feil, R., Allescher, H.-D., Vanderwinden, J.-M., Hofmann, F., Schemann, M. et al. (2013). Interstitial cells of Cajal integrate excitatory and inhibitory neurotransmission with intestinal slow-wave activity. *Nat. Commun.* **4**, 1630.
Klotz, L., Norman, S., Vieira, J. M., Masters, M., Rohling, M., Dubé, K. N., Bollini, S., Matsuzaki, F., Carr, C. A. and Riley, P. R. (2015). Cardiac lymphatics are heterogeneous in origin and respond to injury. *Nature* **522**, 62-67.
Koltowska, K., Lagendijk, A. K., Pichol-Thievend, C., Fischer, J. C., Francois, M., Ober, E. A., Yap, A. S. and Hogan, B. M. (2015). Vegfc regulates bipotential precursor division and Prox1 expression to promote lymphatic identity in zebrafish. *Cell Rep.* **13**, 1828-1841.
Li, W. and Mukouyama, Y. S. (2013). Tissue-specific venous expression of the EPH family receptor EphB1 in the skin vasculature. *Dev. Dyn.* **242**, 976-988.
Madisen, L., Zwingman, T. A., Sunkin, S. M., Oh, S. W., Zariwala, H. A., Gu, H., Ng, L. L., Palmiter, R. D., Hawrylycz, M. J., Jones, A. R. et al. (2010). A robust and high-throughput Cre reporting and characterization system for the whole mouse brain. *Nat. Neurosci.* **13**, 133-140.
Mahadevan, A., Welsh, I. C., Sivakumar, A., Gludish, D. W., Shilvock, A. R., Noden, D. M., Huss, D., Lansford, R. and Kurpios, N. A. (2014). The left-right Pitx2 pathway drives organ-specific arterial and lymphatic development in the intestine. *Dev. Cell* **31**, 690-706.
Martinez-Corral, I., Ulvmar, M. H., Stanczuk, L., Tatin, F., Kizhatil, K., John, S. W. M., Alitalo, K., Ortega, S. and Makinen, T. (2015). Nonvenous origin of dermal lymphatic vasculature. *Circ. Res.* **116**, 1649-1654.
Mcmahon, A. P., Aronow, B. J., Davidson, D. R., Davies, J. A., Gaido, K. W., Grimmond, S., Lessard, J. L., Little, M. H., Potter, S. S., Wilder, E. L. et al. (2008). GUDMAP: the genitourinary developmental molecular anatomy project. *J. Am. Soc. Nephrol.* **19**, 667-671.
Motoike, T., Loughna, S., Perens, E., Roman, B. L., Liao, W., Chau, T. C., Richardson, C. D., Kawate, T., Kuno, J., Weinstein, B. M. et al. (2000). Universal GFP reporter for the study of vascular development. *Genesis* **28**, 75-81.
Mukouyama, Y.-S., Shin, D., Britsch, S., Taniguchi, M. and Anderson, D. J. (2002). Sensory nerves determine the pattern of arterial differentiation and blood vessel branching in the skin. *Cell* **109**, 693-705.
Nicenboim, J., Malkinson, G., Lupo, T., Asaf, L., Sela, Y., Mayseless, O., Gibbs-Bar, L., Senderovich, N., Hashimshony, T., Shin, M. et al. (2015). Lymphatic vessels arise from specialized angioblasts within a venous niche. *Nature* **522**, 56-61.
Ny, A., Koch, M., Schneider, M., Neven, E., Tong, R. T., Maity, S., Fischer, C., Plaisance, S., Lambrechts, D., Héligon, C. et al. (2005). A genetic Xenopus laevis tadpole model to study lymphangiogenesis. *Nat. Med.* **11**, 998-1004.
Okuda, K. S., Astin, J. W., Misa, J. P., Flores, M. V., Crosier, K. E. and Crosier, P. S. (2012). lyve1 expression reveals novel lymphatic vessels and new mechanisms for lymphatic vessel development in zebrafish. *Development* **139**, 2381-2391.
Pham, T. H. M., Baluk, P., Xu, Y., Grigorova, I., Bankovich, A. J., Pappu, R., Coughlin, S. R., Mcdonald, D. M., Schwab, S. R. and Cyster, J. G. (2010). Lymphatic endothelial cell sphingosine kinase activity is required for lymphocyte egress and lymphatic patterning. *J. Exp. Med.* **207**, 17-27.
Sabin, F. R. (1902). On the origin of the lymphatic system from the veins and the development of the lymph hearts and thoracic duct in the pig. *Am. J. Anat.* **1**, 367-389.
Schneider, M., Othman-Hassan, K., Christ, B. and Wilting, J. (1999). Lymphangioblasts in the avian wing bud. *Dev. Dyn.* **216**, 311-319.
Srinivas, S., Watanabe, T., Lin, C.-S., William, C. M., Tanabe, Y., Jessell, T. M. and Costantini, F. (2001). Cre reporter strains produced by targeted insertion of EYFP and ECFP into the ROSA26 locus. *BMC Dev. Biol.* **1**, 4.
Srinivasan, R. S., Dillard, M. E., Lagutin, O. V., Lin, F.-J., Tsai, S., Tsai, M.-J., Samokhvalov, I. M. and Oliver, G. (2007). Lineage tracing demonstrates the venous origin of the mammalian lymphatic vasculature. *Genes Dev.* **21**, 2422-2432.
Srinivasan, R. S., Geng, X., Yang, Y., Wang, Y., Mukatira, S., Studer, M., Porto, M. P. R., Lagutin, O. and Oliver, G. (2010). The nuclear hormone receptor Coup-TFII is required for the initiation and early maintenance of Prox1 expression in lymphatic endothelial cells. *Genes Dev.* **24**, 696-707.
Stanczuk, L., Martinez-Corral, I., Ulvmar, M. H., Zhang, Y., Lavina, B., Fruttiger, M., Adams, R. H., Saur, D., Betsholtz, C., Ortega, S. et al. (2015). cKit lineage hemogenic endothelium-derived cells contribute to mesenteric lymphatic vessels. *Cell Rep.* **10**, 1708-1721.
Tsai, F.-Y., Keller, G., Kuo, F. C., Weiss, M., Chen, J., Rosenblatt, M., Alt, F. W. and Orkin, S. H. (1994). An early haematopoietic defect in mice lacking the transcription factor GATA-2. *Nature* **371**, 221-226.
Uhrin, P., Zaujec, J., Breuss, J. M., Olcaydu, D., Chrenek, P., Stockinger, H., Fuertbauer, E., Moser, M., Haiko, P., Fassler, R. et al. (2010). Novel function for blood platelets and podoplanin in developmental separation of blood and lymphatic circulation. *Blood* **115**, 3997-4005.
Ulvmar, M. H., Martinez-Corral, I., Stanczuk, L. and Mäkinen, T. (2016). Pdgfrb-Cre targets lymphatic endothelial cells of both venous and non-venous origins. *Genesis* **54**, 350-358.
Wang, Y., Nakayama, M., Pitulescu, M. E., Schmidt, T. S., Bochenek, M. L., Sakakibara, A., Adams, S., Davy, A., Deutsch, U., Lüthi, U. et al. (2010). Ephrin-B2 controls VEGF-induced angiogenesis and lymphangiogenesis. *Nature* **465**, 483-486.
Wigle, J. T. and Oliver, G. (1999). Prox1 function is required for the development of the murine lymphatic system. *Cell* **98**, 769-778.
Wilting, J., Aref, Y., Huang, R., Tomarev, S. I., Schweigerer, L., Christ, B., Valasek, P. and Papoutsi, M. (2006). Dual origin of avian lymphatics. *Dev. Biol.* **292**, 165-173.
Yang, Y., Garcia-Verdugo, J. M., Soriano-Navarro, M., Srinivasan, R. S., Scallan, J. P., Singh, M. K., Epstein, J. A. and Oliver, G. (2012). Lymphatic endothelial progenitors bud from the cardinal vein and intersomitic vessels in mammalian embryos. *Blood* **120**, 2340-2348.

SUPPLEMENTAL FIGURES

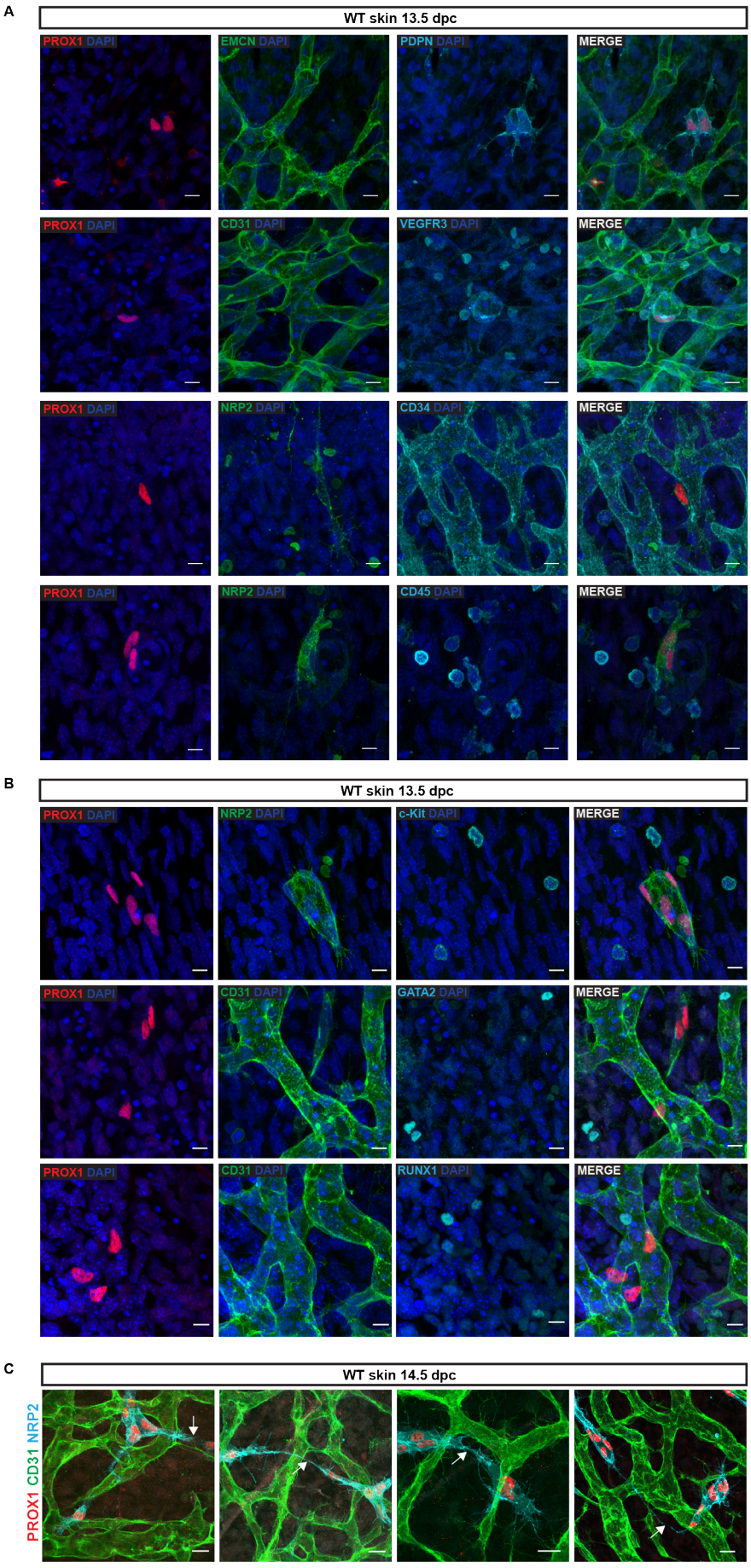

SUPPLEMENTAL FIGURE 1

Supplemental Figure 1: Characterisation of LEC clusters.

(A and B) Whole mount immunostaining of WT skins at 13.5 dpc for indicated proteins. Scale bars, 10 µm. (C) Whole mount immunostaining of WT skins at 14.5 dpc for CD31 (green), PROX1 (red) and NRP2 (blue). Arrows indicate filopodial contact extensions between LEC clusters and between LEC clusters and sprouting vessels. Scale bars, 20 µm. All images correspond to maximum intensity projections.

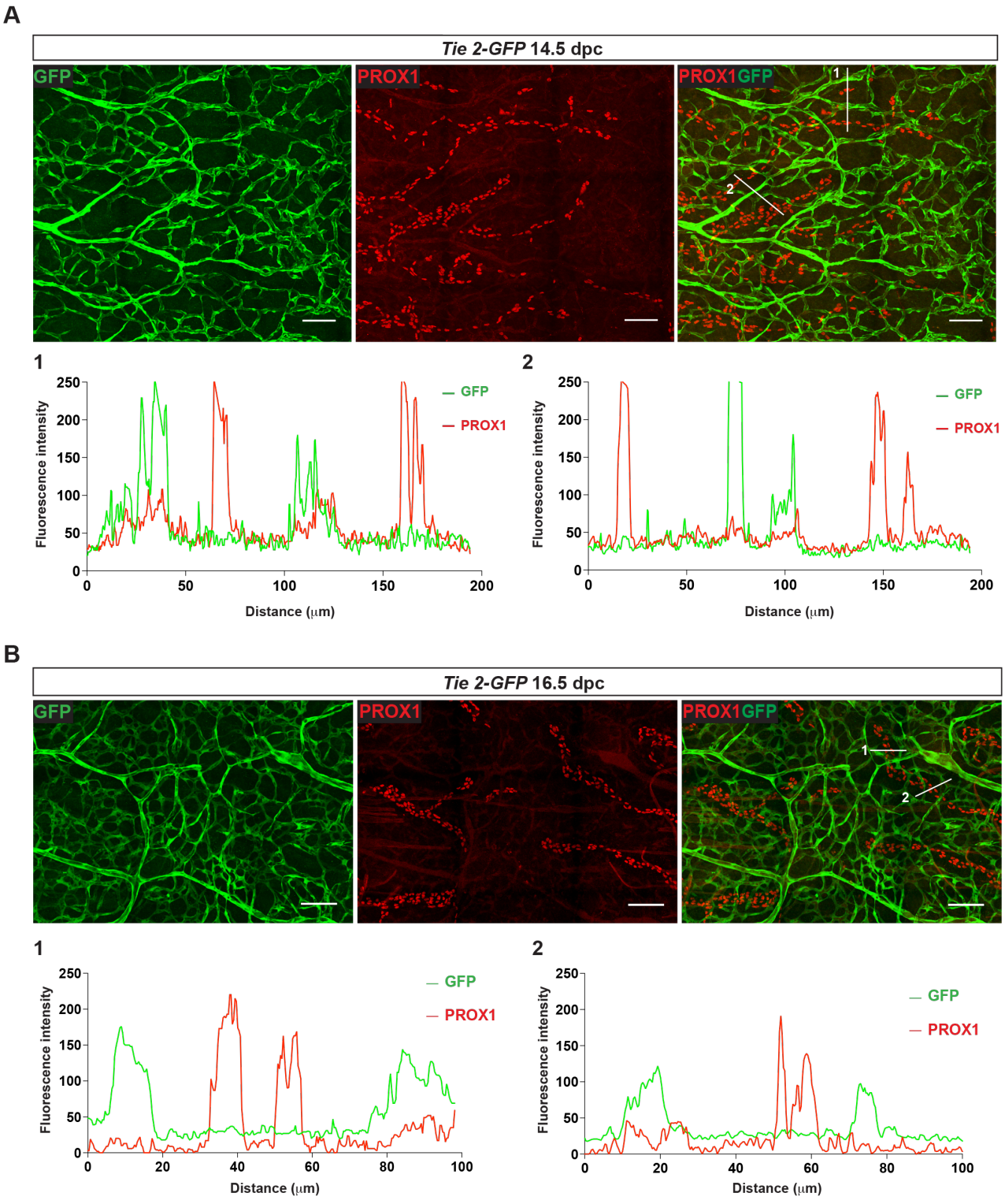

SUPPLEMENTAL FIGURE 2

Supplemental Figure 2: *Tie-2* is not express in dermal LECs.

Whole mount immunostaining of *Tie2-GFP* embryonic skin at 14.5 dpc (A) and 16.5 dpc (B) for PROX1 (red) and GFP (green). Graphs represent the fluorescent intensity of PROX1 and GFP over two independent 200 μm (A) and 100 μm (B) line-regions (1 and 2). GFP is strongly expressed in BECs and not detected in LECs. Scale bars, 100 μm.

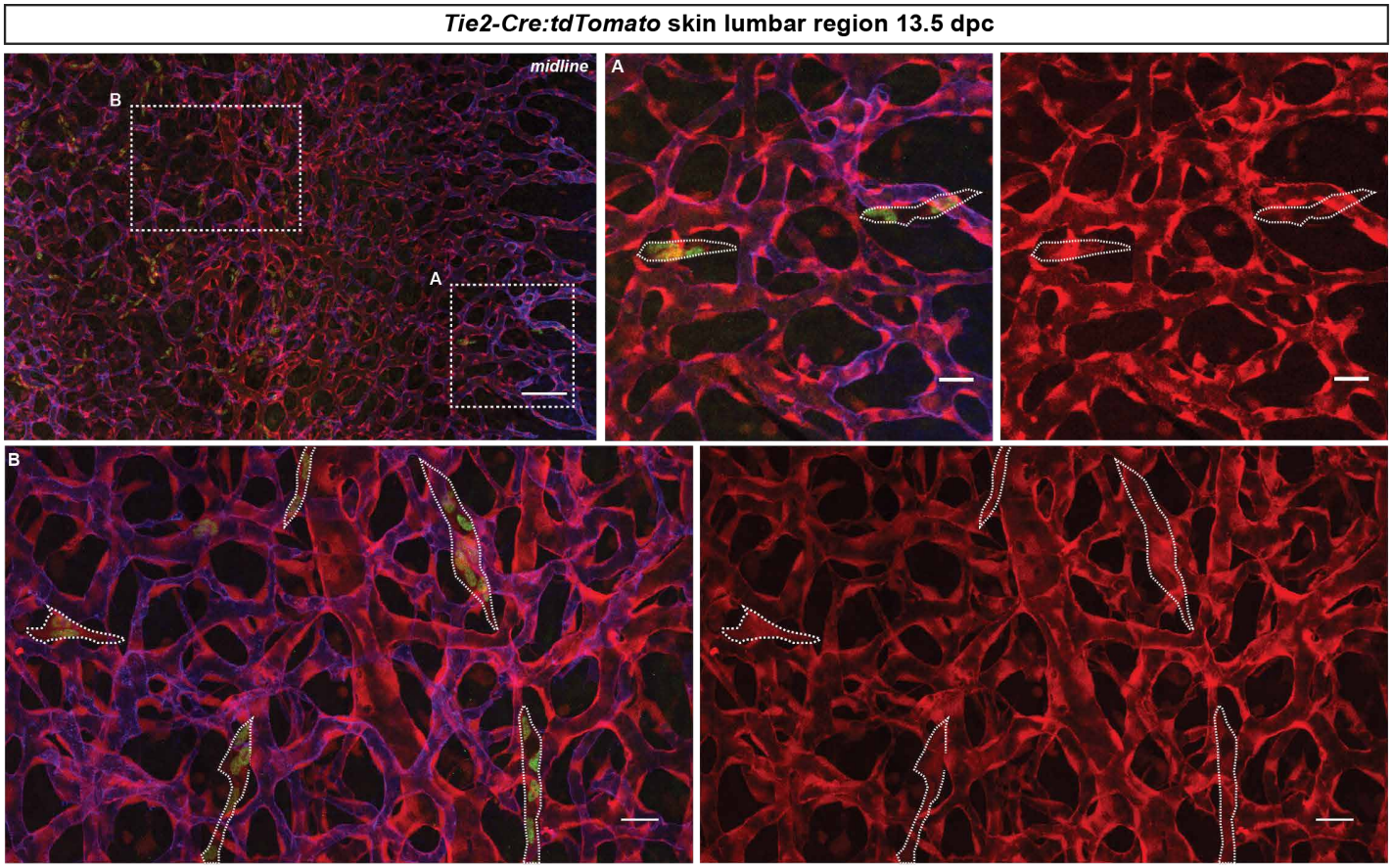

SUPPLEMENTAL FIGURE 3

Supplemental Figure 3: Lumbar LEC clusters have an endothelial origin.

Dermal whole mount immunostaining of *Tie2-Cre:tdTomato* skin (lumbar region) at 13.5 dpc for PROX1 (green) and EMCN (blue). In the lumbar region most LECs are tdTomato-positive. Scale bars 100 μm (top left image), 25 μm (all other images).

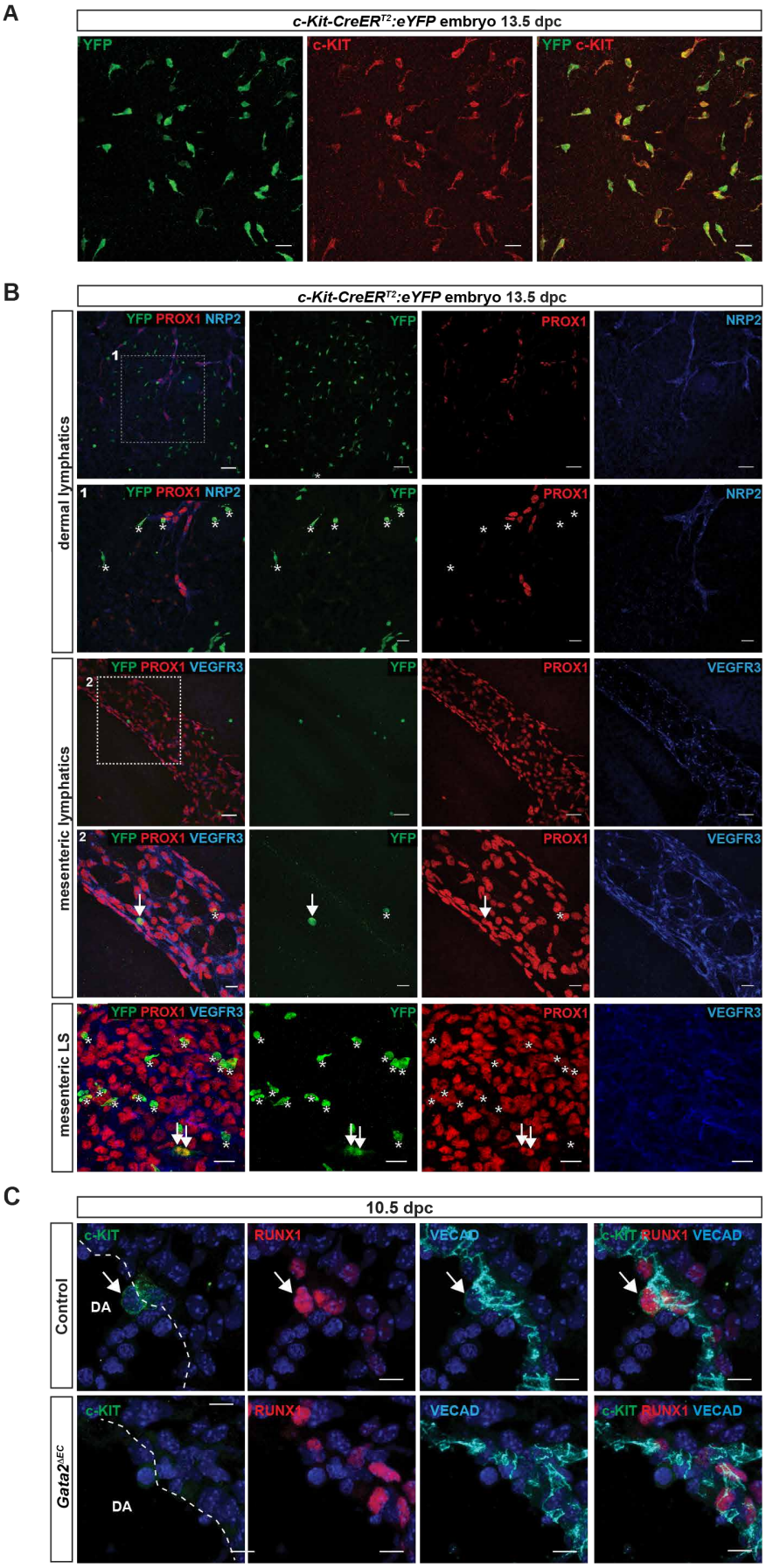

SUPPLEMENTAL FIGURE 4

Supplemental Figure 4: Hemogenic endothelium does not contribute to the formation of dermal lymphatics.

(A) Whole mount immunostaining of *c-Kit-CreERT2:eYFP* skin at 13.5 dpc for YFP (green) and c-KIT (red). YFP-positive cells are found in the skin and still express c-KIT protein. Scale bars, 20 μm (B) Whole mount immunostaining of *c-Kit-CreERT2:eYFP* skin (top) and mesentery (bottom) of the same embryo at 13.5 dpc for YFP (green), PROX1 (red) and NRP2 or VEGFR3 (blue). While scattered YFP-positive cells are found in the mesenteric lymphatic vessels and lymph sac (LS) (arrows), no YFP-positive cells where detected in the dermal lymphatics. Some YFP-positive/PROX1-negative cells are detected in the skin and mesentery (asterisks). In this experiments a single dose of tamoxifen was injected at 10.5 dpc. Boxed regions in upper panels (scale bars, 50 μm) are shown at higher magnification below (scale bars, 20 μm). (C) Transverse sections through the dorsal aorta (DA, dashed region) in the aorta-gonad-mesonephros region at 10.5 dpc stained for the hematopoietic stem cell markers RUNX1 (red) and c-KIT (green). Hematopoietic progenitor cells bud from the wall of the dorsal aorta (top, arrows) in littermate control embryos and are absent from the same region in *Gata2*$^{\Delta EC}$ embryos (bottom). Scale bars, 10 μm.

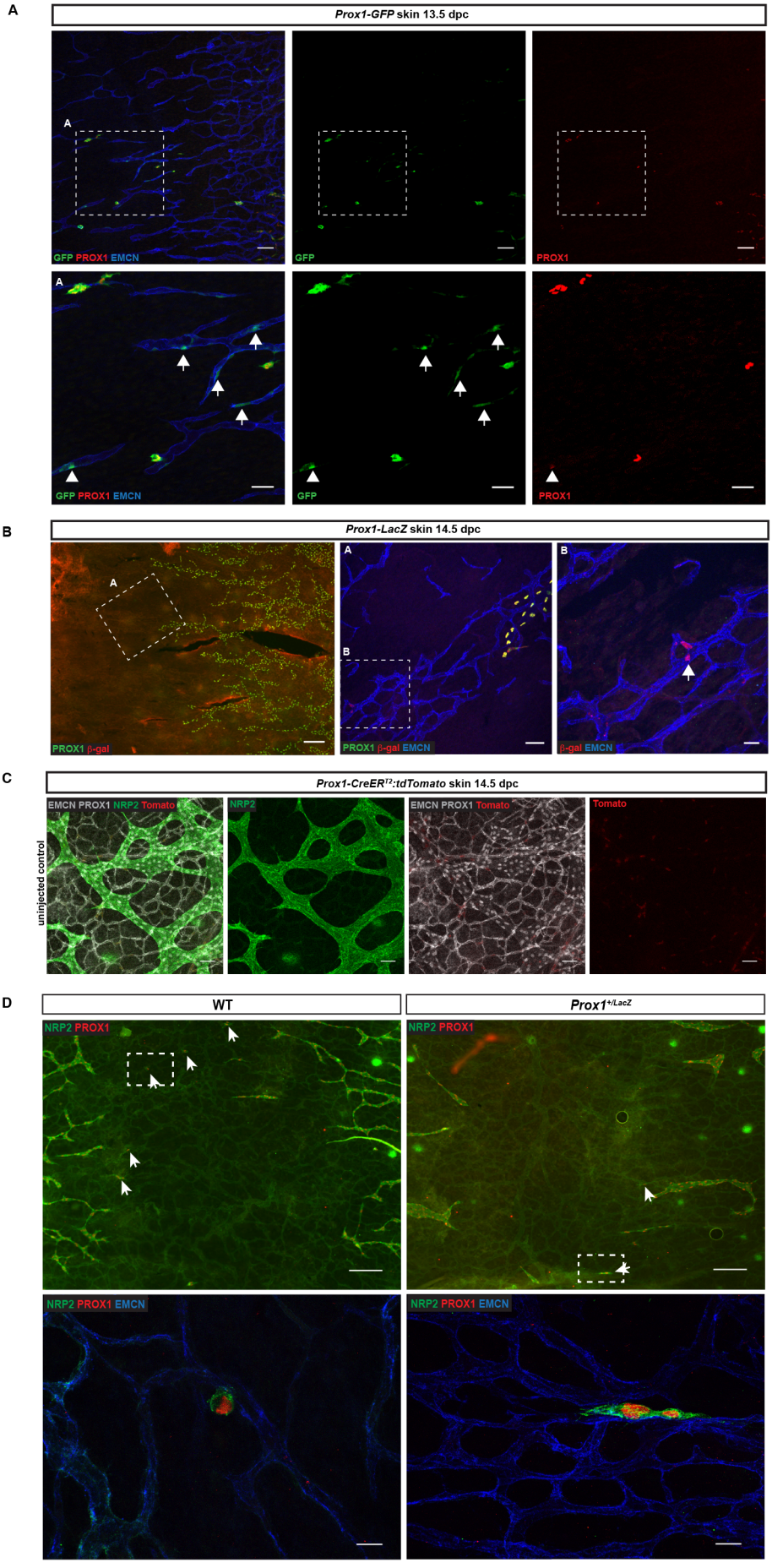

SUPPLEMENTAL FIGURE 5

Supplemental Figure 5: Characterisation of PROX1 expression in the dermal blood vascular capillary plexus. (A) Whole mount immunostaining of *Prox1-GFP* embryonic skin at 13.5 dpc for PROX1 (red), GFP (green) and EMCN (blue). GFP low cells are detected in the blood vascular plexus (arrows). Arrowhead depicts an endothelial cell that is GFP-positive and PROX1 protein low, suggesting the recent induction of PROX1 expression. Boxed regions in upper panels (scale bars, 50 μm) are shown at higher magnification below (scale bars, 20 μm). (B) Whole mount immunostaining of *Prox1-LacZ* embryonic skin at 14.5 dpc for PROX1 (green), β-gal (red) and EMCN (blue). Sparse β-gal-positive cells are detected in the blood vascular plexus (boxed region, arrow). Scale bars, 200 μm (left panel), 50 μm (middle panel), 20 μm (right panel). (C) Whole mount immunostaining of uninjected control *Prox1-CreERT2:tdTomato* skin for PROX1 (grey), EMCN (grey) and NRP2 (green) at 14.5 dpc. Scale bars, 50 μm. (D) Whole mount immunostaining of WT (left) and *Prox1+/LacZ* (right) embryonic skin at 14.5 dpc for PROX1 (red), NRP2 (green) and EMCN (blue). Arrows indicate LEC clusters. Boxed regions in upper panels are shown at higher magnification below. Scale bars, 200 μm (upper panels), 20 μm (lower panels).

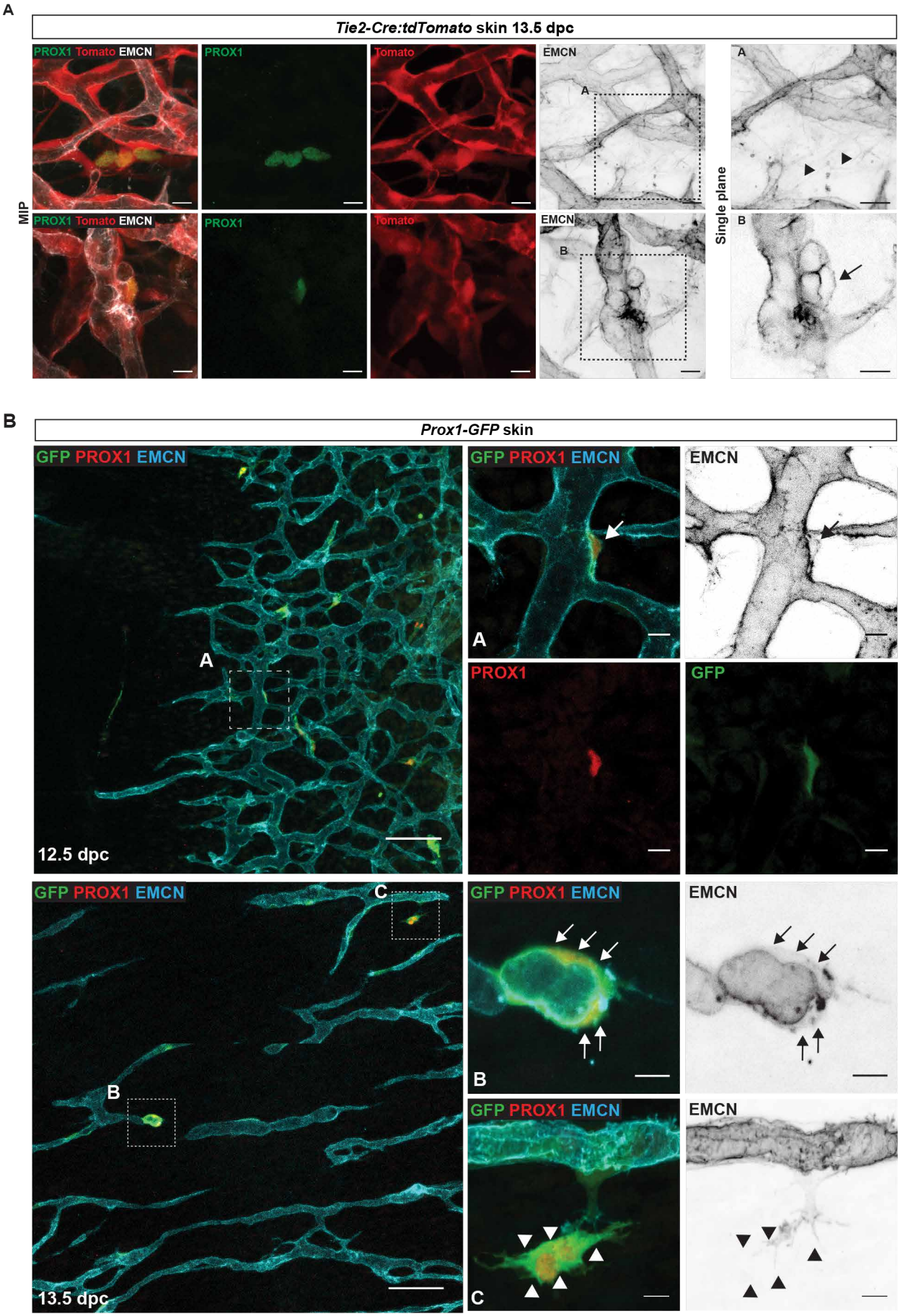

SUPPLEMENTAL FIGURE 6

Supplemental Figure 6: PROX1-positive/Endomucin-positive cells are found in the endothelial lining of the vessel wall. (A) Whole mount immunostaining of *Tie2Cre:tdTomato* skin at 13.5 dpc for PROX1 (green) and Endomucin (grey). While LEC clusters (arrowheads) are not expressing Endomucin (top panel), PROX1-positive cells (arrow) are found in the Endomucin positive plexus. Scale bars, 10 µm (B) Whole mount immunostaining of *Prox1-GFP* embryonic skins at 12.5 (top) and 13.5 dpc (bottom) for EMCN (blue), PROX1 (red) and GFP (green). Endogenous PROX1 is detected in the Endomucin-positive plexus (A and B), while LEC clusters are not expressing Endomucin (C). Boxed regions in left hand panels are shown at higher magnification in right panels. Arrows indicate PROX1-positive/Endomucin-positive cells and arrowheads indicate Endomucin-negative LEC clusters. Scale bars, 100 µm (left panels), 10µm (right panels).

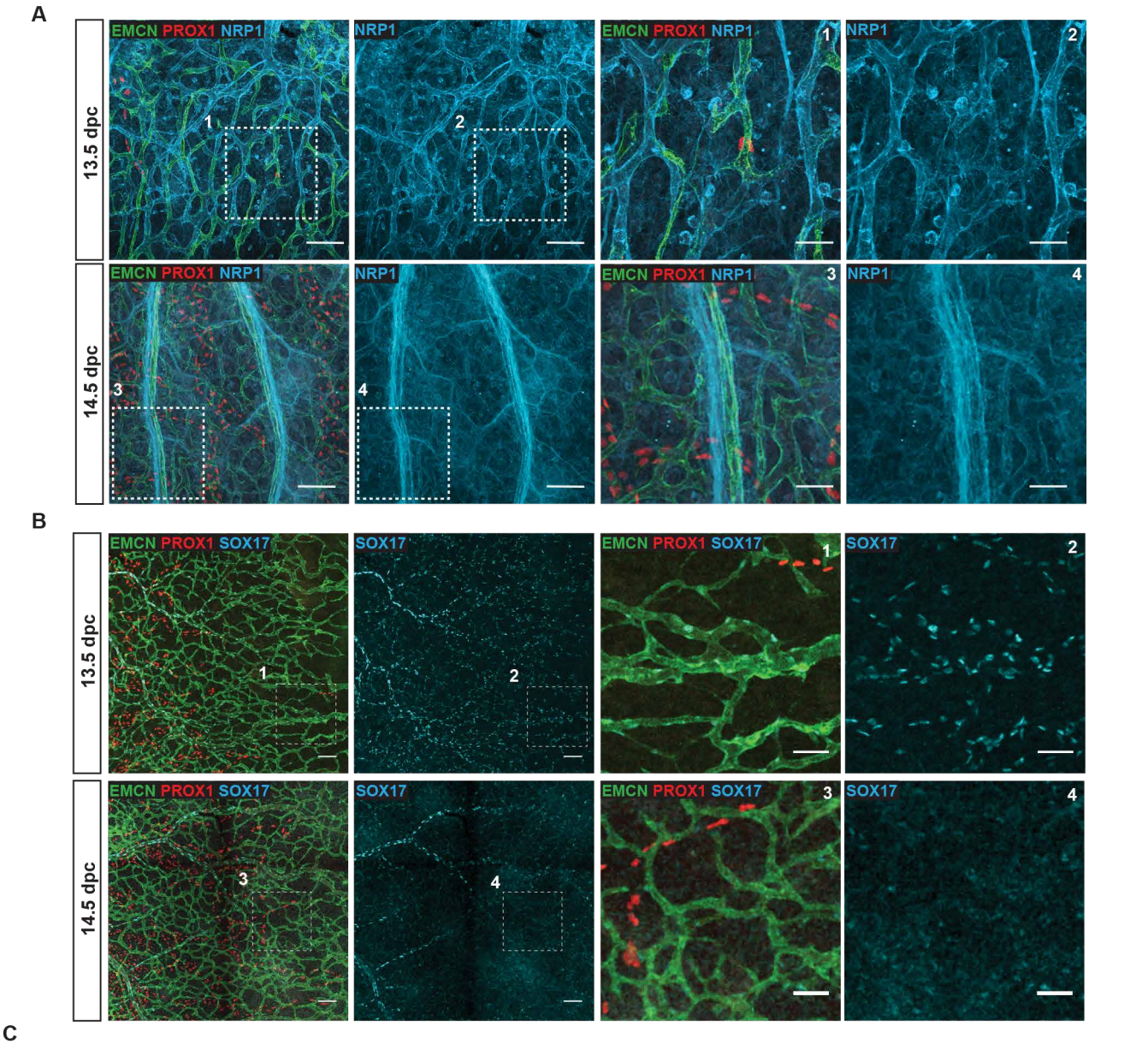

SUPPLEMENTAL FIGURE 7

Supplemental Figure 7: The dermal blood vascular capillary plexus exhibits markers of arterial and venous identity. (A) Whole mount immunostaining of embryonic skin at 13.5 dpc (top) and 14.5 dpc (bottom) for Endomucin (green), NRP1 (blue) and PROX1 (red). Scale bars, 100 μm (left panel), 50 μm (right panel). (B) Whole mount immunostaining of embryonic skin at 13.5 dpc (top) and 14.5 dpc (bottom) for PROX1 (red), Endomucin (green) and SOX17 (blue). Scale bars, 200 μm (left panel), 50 μm (right panel). While NRP1 and SOX17 are broadly expressed in the dermal blood plexus at 13.5 dpc, both arterial markers become restricted to arterioles at 14.5 dpc (A, B) Boxed regions in left panels are shown at higher magnification on right panels. (C) Whole mount immunostaining of embryonic skin at indicated time points for Endomucin (green) and Cx40 (red). Cx40 expression is weakly expressed in the blood vascular plexus at 13.5 dpc (arrows) and restricted to arterioles from 14.5 dpc. Endomucin expression is no longer expressed in arterioles from 15.5 dpc. Scale bars, 50 μm.

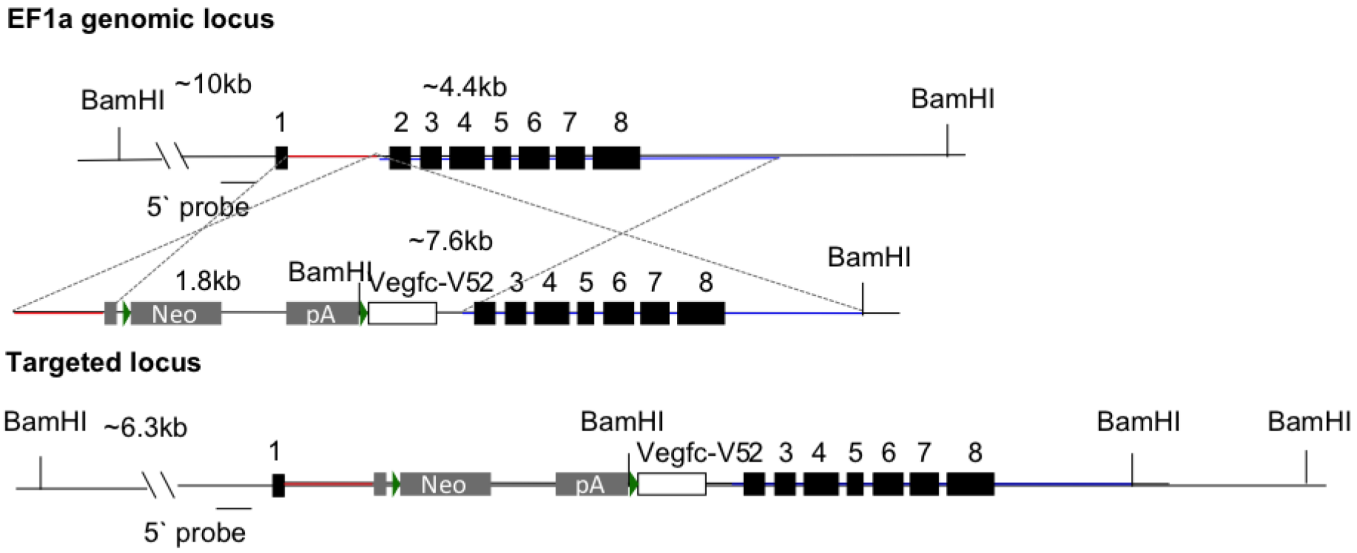

SUPPLEMENTAL FIGURE 8

Supplemental Figure 8: Generation of the *Vegf-cGOF* knock-in strain. The floxP flanked Poly(A) and neomycin cassette was inserted before the full length cDNA of mouse Vegfc with V5 tag. This construct was electroporated into W9.5 embryonic stem cells. The embryonic stem cells were then digested by BamHI, and genotyped by Southern blot analysis using the indicated probes. Correctly targeted embryonic stem cell clones were used to generate chimeric mice at St Jude Children's Research Hospital and Northwestern University.

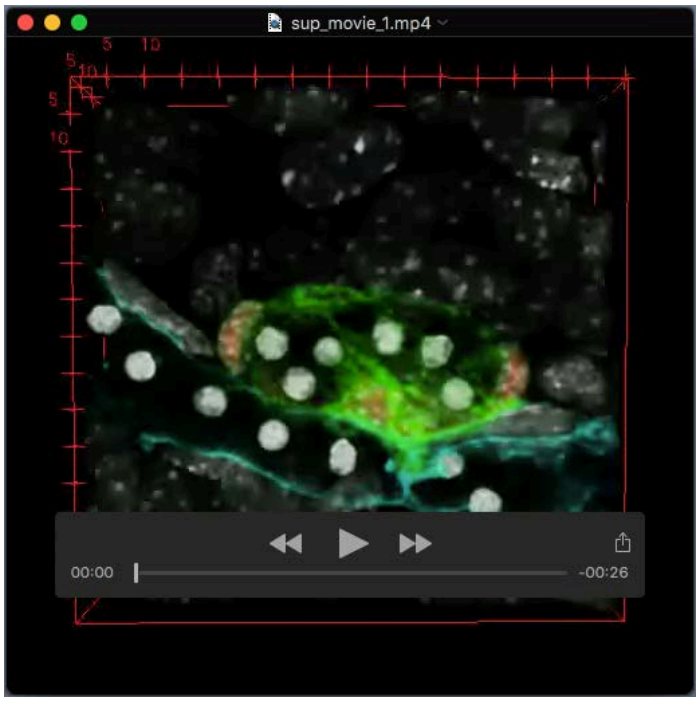

Supplemental Movie 1: Full z-stack images shown in Figure 5A. 3D volume rendering for Endomucin (blue), PROX1 (red), NRP2 (green) and DAPI allowing visualisation of the multicellular cluster that is budding from the Endomucin-positive blood vessel. Red blood cells are embedded inside the LEC cluster that still remains connected to the adjacent blood vessel.

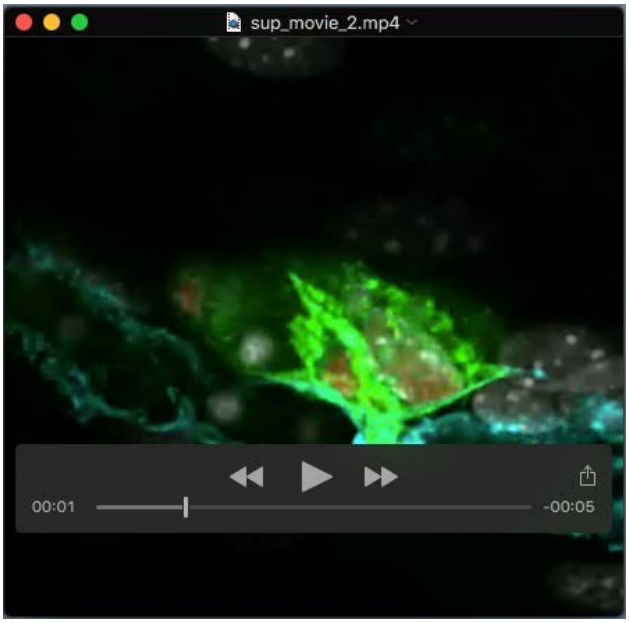

Supplemental Movie 2: Full z-stack images shown in Figure 5A.